

# **PNNL's Characterization Summary for the MP-2 Experiment**

December 2022

Rajib Kalsar  
Benjamin J Schuessler  
Ayoub Soulami  
Vineet V Joshi

## DISCLAIMER

This report was prepared as an account of work sponsored by an agency of the United States Government. Neither the United States Government nor any agency thereof, nor Battelle Memorial Institute, nor any of their employees, **makes any warranty, express or implied, or assumes any legal liability or responsibility for the accuracy, completeness, or usefulness of any information, apparatus, product, or process disclosed, or represents that its use would not infringe privately owned rights.** Reference herein to any specific commercial product, process, or service by trade name, trademark, manufacturer, or otherwise does not necessarily constitute or imply its endorsement, recommendation, or favoring by the United States Government or any agency thereof, or Battelle Memorial Institute. The views and opinions of authors expressed herein do not necessarily state or reflect those of the United States Government or any agency thereof.

PACIFIC NORTHWEST NATIONAL LABORATORY  
*operated by*  
BATTELLE  
*for the*  
UNITED STATES DEPARTMENT OF ENERGY  
*under Contract DE-AC05-76RL01830*

Printed in the United States of America

Available to DOE and DOE contractors from  
the Office of Scientific and Technical  
Information,  
P.O. Box 62, Oak Ridge, TN 37831-0062  
[www.osti.gov](http://www.osti.gov)  
ph: (865) 576-8401  
fox: (865) 576-5728  
email: [reports@osti.gov](mailto:reports@osti.gov)

Available to the public from the National Technical Information Service  
5301 Shawnee Rd., Alexandria, VA 22312  
ph: (800) 553-NTIS (6847)  
or (703) 605-6000  
email: [info@ntis.gov](mailto:info@ntis.gov)  
Online ordering: <http://www.ntis.gov>

# **PNNL's Characterization Summary for the MP-2 Experiment**

**December 2022**

Rajib Kalsar  
Benjamin J Schuessler  
Ayoub Soulami  
Vineet V Joshi

Prepared for  
the U.S. Department of Energy  
under Contract DE-AC05-76RL01830

Pacific Northwest National Laboratory  
Richland, Washington 99354

## DISCLAIMER

This report was prepared as an account of work sponsored by an agency of the United States Government. Neither the United States Government nor any agency thereof, nor Battelle Memorial Institute, nor any of their employees, makes **any warranty, express or implied, or assumes any legal liability or responsibility for the accuracy, completeness, or usefulness of any information, apparatus, product, or process disclosed, or represents that its use would not infringe privately owned rights.** Reference herein to any specific commercial product, process, or service by trade name, trademark, manufacturer, or otherwise does not necessarily constitute or imply its endorsement, recommendation, or favoring by the United States Government or any agency thereof, or Battelle Memorial Institute. The views and opinions of authors expressed herein do not necessarily state or reflect those of the United States Government or any agency thereof.

PACIFIC NORTHWEST NATIONAL LABORATORY

*operated by*

BATTELLE

*for the*

UNITED STATES DEPARTMENT OF ENERGY

*under Contract DE-AC05-76RL01830*

**Printed in the United States of America**

**Available to DOE and DOE contractors from the**

**Office of Scientific and Technical Information,**

**P.O. Box 62, Oak Ridge, TN 37831-0062;**

**ph: (865) 576-8401**

**fax: (865) 576-5728**

**email: [reports@adonis.osti.gov](mailto:reports@adonis.osti.gov)**

**Available to the public from the National Technical Information Service**

**5301 Shawnee Rd., Alexandria, VA 22312**

**ph: (800) 553-NTIS (6847)**

**email: [orders@ntis.gov](mailto:orders@ntis.gov) <<http://www.ntis.gov/about/form.aspx>>**

**Online ordering: <http://www.ntis.gov>**



This document was printed on recycled paper.

(8/2010)

## Summary

Characterization of as-fabricated fuel was performed at Pacific Northwest National Laboratory (PNNL) in accordance with the characterization plan for the fabrication of U-10Mo plate fuel for the U.S. High Performance Research Reactor conversion program's Fuel Fabrication Pillar (INL 2021). Similar characterization work is also being performed at Idaho National Laboratory to provide a detailed understanding of the as-fabricated foils that would be irradiated in the Mini-Plate 2 (MP-2) experiment. Under the MP-2 characterization plan, foils are studied that have different fabrication parameters (such as rolling condition, rolling thickness reduction, co-rolling with Zr layers). Similar samples from master foils were sent to both the organizations, so that the testing and analysis can be done independently using similar equipment and standardized measurement and analysis procedures. A final, consolidated report will be prepared based on this work and will summarize all the information obtained from the two laboratories. The MP-2 experiment will provide an opportunity to understand the effects of processing conditions on the final fuel microstructure, to compare results obtained independently, and achieve a two-way validation. In Fiscal Year 2022, PNNL received five MP-2 cast (PD-STD2)<sup>1</sup> samples to examine the foils' chemistry and microstructure. For cast sample, PNNL received samples from three different locations for each cast plate. PNNL also received and characterized 24 U-10Mo foil samples, by sectioning four pieces/specimens from each foil, in accordance with the MP-2 Characterization Plan (INL 2021). These 24 samples consist of three types of foils from BWX Technologies: 0.047 in. thick hot-rolled and annealed samples with Zr layers; 0.025 in. thick cold-rolled and annealed samples with Zr layers; 0.0105 in. thick cold-rolled and annealed samples with Zr layers. Along with these, PNNL also received four large foils with Zr layers that were 0.025 in. and 0.0105 in. thick. This report describes the results of PNNL's MP-2 foil characterization. Microstructure, Mo homogeneity, carbide fraction and morphology, U-10Mo foil thickness, and Zr thickness were evaluated in both the longitudinal and transverse directions for all the foils of the three different thicknesses.

---

<sup>1</sup> PD-STD2 is Process Design Standard 2

## Acknowledgments

This work was funded by the U.S. Department of Energy National Nuclear Security Administration's Office of Material Management and Minimization and was performed at Pacific Northwest National Laboratory under contract DE-AC05-76RL01830. The authors thank Mark Rhodes, Jesse Lang, Sulaiman Sannoh, and Alan Schemer-Kohrn for their support in specimen preparation, metallography, and scanning electron microscopy.

## Acronyms and Abbreviations

BSE	backscattered electron
BWXT	BWX Technologies
EBSD	electron backscatter diffraction
EDS	energy-dispersive x-ray spectroscopy
HIP	hot isostatic press
INL	Idaho National Laboratory
LABE	low-angle backscattered electron
LEI	lower electron image
LEU	low-enriched uranium
MP-2	Mini-Plate 2 experiment
PD-STD2	Process Design Standard 2
PNNL	Pacific Northwest National Laboratory
SD	standard deviation
SDD	silicon drift detector
SEI	secondary electron imaging
SEM	scanning electron microscopy
UC	uranium carbide
WDS	wavelength-dispersive x-ray spectroscopy
Y-12	DOE's Y-12 National Security Complex in Oak Ridge, Tennessee

## Contents

Summary.....	ii
Acknowledgments.....	iii
Acronyms and Abbreviations .....	iv
1.0 Introduction .....	1
2.0 Materials.....	2
3.0 Specimen Preparation.....	5
3.1 Specimen Sectioning.....	5
3.2 Specimen Mounting, Grinding, and Polishing.....	9
3.3 Heat Treatment of As-Cast Specimens .....	9
4.0 Equipment Used for Analysis .....	10
4.1 Optical Microscope .....	10
4.2 Scanning Electron Microscope .....	10
4.3 Electron Backscatter Diffraction .....	12
5.0 Results and Discussion .....	13
5.1 Grain Size.....	13
5.1.1 Grain Size Measurement Using Optical Microscope .....	13
5.1.2 Grain Size Measurements Using EBSD .....	17
5.2 Molybdenum Distribution and Chemical Banding.....	18
5.3 Carbide Fraction and Size Evaluation .....	22
5.4 Gamma Phase Decomposition.....	29
5.5 Fuel Meat Thickness .....	30
5.6 Zr Layer Thickness .....	31
6.0 Conclusions.....	37
7.0 Quality Assurance .....	39
8.0 References.....	40

## Figures

Figure 1.	Sectioning diagram according to the Characterization Plan for the Fabrication of U-10Mo Plate Fuel for U.S. High Performance Research Reactors .....	8
Figure 2.	Representative center-montage images of U-10Mo specimens with different thicknesses.....	11
Figure 3.	Representative microstructures of cast specimens .....	13
Figure 4.	Representative microstructures of foil specimens with different thicknesses.....	15

Figure 5.	Representative microstructures of plate specimens with different thicknesses.....	15
Figure 6.	EBSD-generated microstructures of U-10Mo specimens.....	17
Figure 7.	Grain size distribution calculated from EBSD microstructures for LEU2051, LEU2021, and LEU2036.....	18
Figure 8.	Mo distribution (along a line scan across the specimen thickness) for a U-10Mo specimen of thickness 0.047 in.....	20
Figure 9.	BSE-SEM microstructures of U-10Mo specimens of thickness 0.01 in. ....	23
Figure 10.	Schematic illustration of steps performed while using ImageJ analysis software.....	24
Figure 11.	BSE-SEM microstructures of U-10Mo specimens of thickness 0.01 in. after ImageJ thresholding.....	24
Figure 12.	Summary plots of carbide analysis for as-cast and foil samples.....	27
Figure 13.	Typical Zr layers observed in U-10Mo foil specimens.....	32
Figure 14.	Typical Zr layers observed in U-10Mo large foil specimens.....	32
Figure 15.	Zr thickness variation of Zr layer thickness with thickness reduction.....	36
Figure 16.	Representative interaction layers observed in U-10Mo specimens.....	36
Figure 17.	Average grain size ranges for different thickness U-10Mo master foils, and 0.025 in. and 0.010 in. thick foils.....	37

## Tables

Table 1.	U-10Mo MP-2 characterization of cast samples analyzed at PNNL.....	2
Table 2.	U-10Mo hot-rolled, cold-rolled and annealed MP-2 samples from Lot 054.....	3
Table 3.	U-10Mo hot-rolled, cold-rolled and annealed MP-2 samples from Lot 055.....	3
Table 4.	U-10Mo hot-rolled, cold-rolled and annealed MP-2 samples from large foils.....	4
Table 5.	U10Mo MP2 characterization specimens analyzed at PNNL.....	5
Table 6.	U-10Mo MP-2 cast samples characterized and analyzed at PNNL.....	5
Table 7.	U-10Mo MP-2 characterization of cast + homogenized samples analyzed at PNNL.....	5
Table 8.	U-10Mo hot-rolled, cold-rolled and annealed MP-2 samples from Lot 054.....	6
Table 9.	U-10Mo hot-rolled, cold-rolled and annealed MP-2 samples from Lot 055.....	6
Table 10.	U-10Mo MP-2 samples from large foils.....	7
Table 11.	EBSD phase details used for phase indexing.....	12
Table 12.	Grain size of U-10Mo cast and cast + homogenized specimens.....	14
Table 13.	Grain sizes of U-10Mo specimens obtained by optical microscopy.....	16
Table 14.	Mo distribution (EDS measurements) in U-10Mo as-cast and as-cast + homogenized specimens.....	20
Table 15.	Mo distribution (EDS measurements) in U-10Mo foil specimens.....	21
Table 16.	Carbide area fraction in cast and cast + homogenized U-10Mo specimens.....	25

Table 17.	Carbide area fraction in U-10Mo foil specimens.....	25
Table 18.	Carbide particle size in U-Mo cast and cast + homogenized specimens .....	27
Table 20.	Fuel meat thickness of U-10Mo specimens.....	30
Table 21.	Summary of the Zr layer (top and bottom) thicknesses for U-10Mo specimens .....	34

## 1.0 Introduction

The purpose of the Mini-Plate-2 (MP-2) experiment is to demonstrate and verify the fabrication process for co-rolled U-10Mo monolithic fuel that will be implemented at the commercial fabricator to produce materials that meet requirements for commercial viability and irradiation performance.

In the MP-2 test, several mini-plates will be irradiated at various locations in the Idaho National Laboratory's (INL's) Advanced Test Reactor. In the case of the MP-2 irradiation experiment, the extent of the manufacturing needed to produce enough MP-2 plates provide sufficient process data and opportunities for extensive characterization. To effectively begin this investigation, new developments in fabrication of the fuel elements were initiated, yielding a better understanding of the material behavior before and after irradiation. Fabricating the U-10Mo involves material processing techniques such as casting, homogenization, hot and cold rolling, co-rolling, and hot isostatic pressing (HIP). It is very important to correlate the processing with structure and properties. Thus, the variation in the fuel microstructure and processing data can be gathered to better understand the effects of fabrication processes on the U-10Mo monolithic fuel. The MP-2 experiment presents the first opportunity to investigate the microstructure evolution throughout a commercial fabrication process.

Characterization of the as-fabricated fuel was performed at Pacific Northwest National Laboratory (PNNL) according to the characterization plan for the fabrication of U-10Mo plate fuel for the U.S. High Performance Research Reactor (USHPRR) conversion program's Fuel Fabrication Pillar (INL 2021). Similar characterization work is also being performed at INL to provide a detailed understanding of the as-fabricated fuel that would be irradiated in the MP-2 experiment. Under the MP-2 Characterization Plan, fuel foils produced with different fabrication parameters are being studied. Similar samples from master foils were sent to PNNL and INL so that testing and analysis can be performed independently using similar equipment and a standardized set of measurement and analysis procedures. The MP-2 experiment will provide an opportunity to understand the effects of processing conditions on the final fuel microstructure, compare results obtained independently, and achieve a two-way validation.

In accordance with the MP-2 characterization plan (INL 2021), PNNL will analyze the microstructure, chemical composition, carbide fraction and morphology, U-10Mo foil thickness and Zr layer thickness of U-10Mo MP-2 foils received from BWX Technologies (BWXT). The MP-2 experiment presents the first opportunity to investigate the microstructure evolution throughout the fabrication process, from cast to foils. This work will provide insights into the variation in the fuel microstructure and processing data, and eventually can be used to predict yields.

## 2.0 Materials

PNNL received three MP-2 (Process Design Standard 2, PD-STD2) cast samples from the Y-12 National Security Complex (Y-12). Cast sample identification information is given in Table 1. These are the cast samples used for master foils and foil fabrication.

PNNL also received three types of MP-2 foils from BWXT, as shown in Table 2 and Table 3: 0.047 in. hot-rolled and annealed samples with Zr layers; 0.027 in. cold-rolled and annealed samples with Zr layers; and 0.0105 in. cold-rolled and annealed samples with Zr layers. Characterization studies were performed on 20 U-10Mo samples in accordance with the MP-2 Characterization Plan (INL 2021). Additional information about each sample and its condition is shown in Table 2–Table 3.

Apart from the small foils, we also received four large foils, two 0.027 in. thick and two 0.0105 in. thick with Zr layers received from BWXT. The identification details of the large foils are given in Table 4.

Upon receipt of each sample, an entry was made in the Sample Log. The Sample Log contains the sample identification number, sample description, and other relevant information to support positive sample identity and traceability.

Table 1. U-10Mo MP-2 characterization of cast samples analyzed at PNNL

No.	Casting	Sample ID	Locations in cast plate
1	PD-STD2	3L50-CC-1N14	4, 3, 1
2	PD-STD2	3L50-CC-2N14	4, 3, 1
3	PD-STD2	3L50-CC-2N15	4, 3, 1

Table 2. U-10Mo hot-rolled, cold-rolled and annealed MP-2 samples from Lot 054

No.	Y-12 Casting Standard	Ingot	Master Foil	Foil	Foil Area Sample Region	Sample ID	Thickness (in.)
1	PD-STD2	3L50-NN-2N14	054-01-000	N/A	Leading edge	054-01-000 L	0.047
2	PD-STD2	3L50-NN-2N14	054-01-000	N/A	Middle	054-01-000 M	0.047
3	PD-STD2	3L50-NN-1N14	054-02-000	N/A	Leading edge	054-02-000 L	0.047
4	PD-STD2	3L50-NN-1N14	054-02-000	N/A	Middle	054-02-000 M	0.047
5	PD-STD2	3L50-TT-2N14	054-03-000	N/A	Leading edge	054-03-000 L	0.047
6	PD-STD2	3L50-TT-2N14	054-03-000	N/A	Middle	054-03-000 M	0.047
7	PD-STD2	3L50-NN-1N14	054-01-000	054-01-001	Leading edge	054-01-001 L	0.028
8	PD-STD2	3L50-NN-1N14	054-01-000	054-01-002	Middle	054-01-002 M	0.028
9	PD-STD2	3L50-TT-1N14	054-02-000	054-02-001	Leading edge	054-02-001 L	0.028
10	PD-STD2	3L50-TT-1N14	054-02-000	054-02-002	Middle	054-02-002 M	0.028
11	PD-STD2	3L50-TT-2N14	054-03-000	054-03-001	Leading edge	054-03-001 L	0.028
12	PD-STD2	3L50-TT-2N14	054-03-000	054-03-002	Middle	054-03-002 M	0.028

Table 3. U-10Mo hot-rolled, cold-rolled and annealed MP-2 samples from Lot 055

No.	Y-12 Casting Standard	Ingot	Master Foil	Foil	Foil Area Sample Region	Sample ID	Thickness (in.)
1	PD-STD2	3L50-NN-2N14	055-01-000	N/A	Leading edge	055-01-000 L	0.047
2	PD-STD2	3L50-NN-2N14	055-01-000	N/A	Middle	055-01-000 M	0.047
3	PD-STD2	3L50-NN-2N15	055-02-000	N/A	Leading edge	055-02-000 L	0.047
4	PD-STD2	3L50-NN-2N15	055-02-000	N/A	Middle	055-02-000 M	0.047
5	PD-STD2	3L50-NN-2N14	055-01-000	055-01-001	Leading edge	055-01-001 L	0.010
6	PD-STD2	3L50-NN-2N14	055-01-000	055-01-002	Middle	055-01-002 M	0.010
7	PD-STD2	3L50-NN-2N15	055-02-000	055-02-001	Leading edge	055-02-001 L	0.010
8	PD-STD2	3L50-NN-2N15	055-02-000	055-02-001	Middle	055-02-001 M	0.010

Table 4. U-10Mo hot-rolled, cold-rolled and annealed MP-2 samples from large foils

No.	Y-12 Casting Standard	Ingot	Foil	Sample ID	Thickness (in.)
1	PD-STD2	3L50-TT-1N14	1MP-20.027	1MP-20.027	0.025
2	PD-STD2	3L50-TT-1N14	2MP-20.027	2MP-20.027	0.025
3	PD-STD2	3L50-NN-2N15	1MP-20.0105	1MP-20.0105	0.0105
4	PD-STD2	3L50-NN-2N15	2MP-20.0105	2MP-20.0105	0.0105

## 3.0 Specimen Preparation

### 3.1 Specimen Sectioning

The details about the total number of specimens (casting, foils, large foils) we received and the number of metallographic samples we made are given in Table 5. Specimen sectioning from U-10Mo samples listed in Table 6—**Error! Reference source not found.** was performed in accordance with the MP-2 Characterization Plan (INL 2021). Four specimens from each sample were sectioned as follows: two specimens (longitudinal, referred to as L; transverse, referred to as T) from each location (leading edge and middle), as shown in Figure 1 and Table 8—**Error! Reference source not found.** Upon sectioning each sample, an entry was made in the Sample Log. The Sample Log contains the specimen identification number, sample description, and other relevant information to support positive specimen identity and traceability. Heat treatments were performed on selected cast samples. Sample details for heat-treated cast samples are shown in Table 7.

Table 5. U10Mo MP2 characterization specimens analyzed at PNNL

No.	Processed Condition	Foil Thickness (in.)	Ingot/Foil Quantity	Number of Met Specimens
1	Cast samples		3	9
2	Hot-rolled and annealed; co-rolled with Zr	0.047	10	20
3	Cold-rolled; annealed; co-rolled with Zr	0.025	6	12
4	Cold-rolled; annealed; co-rolled with Zr	0.0105	4	8
5	Large foil; co-rolled with Zr	0.027	2	8
6	Large foil; co-rolled with Zr	0.0105	2	8
Total number			27	65

Table 6. U-10Mo MP-2 cast samples characterized and analyzed at PNNL

No.	Casting Standard	Sample ID	Locations	Metallography IDs
1	PD-STD2	3L50-CC-1N14	4, 3, 1	LEU2093, LEU2094, LEU2095
2	PD-STD2	3L50-CC-2N14	4, 3, 1	LEU2099, LEU2100, LEU2101
3	PD-STD2	3L50-CC-2N15	4, 3, 1	LEU2102, LEU2103, LEU2104

Table 7. U-10Mo MP-2 characterization of cast + homogenized samples analyzed at PNNL

No.	Casting Standard	Sample ID	Location	Met IDs
1	PD-STD2	3L50-CC-1N14	1	LEU2112
2	PD-STD2	3L50-CC-2N14	1	LEU2116
3	PD-STD2	3L50-CC-2N15	1	LEU2117

Table 8. U-10Mo hot-rolled, cold-rolled and annealed MP-2 samples from Lot 054

No.	Y-12 Casting Standard	Ingot	Master Foil	Foil	Foil Area Sample Region	Sample ID	Thickness (in.)	Met IDs
1	PD-STD2	3L50-NN-2N14	054-01-000	N/A	Leading edge	054-01-000 L	0.047	LEU2030, LEU2031
2	PD-STD2	3L50-NN-2N14	054-01-000	N/A	Middle	054-01-000 M	0.047	LEU2032, LEU2033
3	PD-STD2	3L50-NN-1N14	054-02-000	N/A	Leading edge	054-02-000 L	0.047	LEU2034, LEU2035
4	PD-STD2	3L50-NN-1N14	054-02-000	N/A	Middle	054-02-000 M	0.047	LEU2043, LEU2044
5	PD-STD2	3L50-TT-2N14	054-03-000	N/A	Leading edge	054-03-000 L	0.047	LEU2047, LEU2048
6	PD-STD2	3L50-TT-2N14	054-03-000	N/A	Middle	054-03-000 M	0.047	LEU2045, LEU2046
7	PD-STD2	3L50-NN-1N14	054-01-000	054-01-001	Leading edge	054-01-001 L	0.028	LEU2018, LEU2021
8	PD-STD2	3L50-NN-1N14	054-01-000	054-01-002	Middle	054-01-002 M	0.028	LEU2024, LEU2025
9	PD-STD2	3L50-TT-1N14	054-02-000	054-02-001	Leading edge	054-02-001 L	0.028	LEU2026, LEU2027
10	PD-STD2	3L50-TT-1N14	054-02-000	054-02-002	Middle	054-02-002 M	0.028	LEU2028, LEU2029
11	PD-STD2	3L50-TT-2N14	054-03-000	054-03-001	Leading edge	054-03-001 L	0.028	LEU2019, LEU2022
12	PD-STD2	3L50-TT-2N14	054-03-000	054-03-002	Middle	054-03-002 M	0.028	LEU2020, LEU2023

Table 9. U-10Mo hot-rolled, cold-rolled and annealed MP-2 samples from Lot 055

No.	Y-12 Casting Standard	Ingot	Master Foil	Foil	Foil Area Sample Region	Sample ID	Thickness (in.)	Met ID
1	PD-STD2	3L50-NN-2N14	055-01-000	N/A	Leading edge	055-01-000 L	0.047	LEU2051, LEU2052
2	PD-STD2	3L50-NN-2N14	055-01-000	N/A	Middle	055-01-000 M	0.047	LEU2053, LEU2055
3	PD-STD2	3L50-NN-2N15	055-02-000	N/A	Leading edge	055-02-000 L	0.047	LEU2068, LEU2070
4	PD-STD2	3L50-NN-2N15	055-02-000	N/A	Middle	055-02-000 M	0.047	LEU2067, LEU2069
5	PD-STD2	3L50-NN-2N14	055-01-000	055-01-001	Leading edge	055-01-001 L	0.010	LEU2036, LEU2037
6	PD-STD2	3L50-NN-2N14	055-01-000	055-01-002	Middle	055-01-002 M	0.010	LEU2049, LEU2050
7	PD-STD2	3L50-NN-2N15	055-02-000	055-02-001	Leading edge	055-02-001 L	0.010	LEU2057, LEU2058
8	PD-STD2	3L50-NN-2N15	055-02-000	055-02-001	Middle	055-02-001 M	0.010	LEU2054, LEU2056

Table 10. U-10Mo MP-2 samples from large foils

No.	Y-12 Casting Standard	Ingot	Large foil	Sample ID	Thickness (in.)	Met ID
1	PD-STD2	3L50-TT-1N14	1MP-20.027	1MP-20.027	0.025	LEU2071, LEU2072, LEU2073, LEU2074
2	PD-STD2	3L50-TT-1N14	2MP-20.027	2MP-20.027	0.025	LEU2075, LEU2076, LEU2077, LEU2078
3	PD-STD2	3L50-NN-2N15	1MP-20.0105	1MP-20.0105	0.0105	LEU2083, LEU2084, LEU2085, LEU2086
4	PD-STD2	3L50-NN-2N15	2MP-20.0105	2MP-20.0105	0.0105	LEU2079, LEU2080, LEU2081, LEU2082

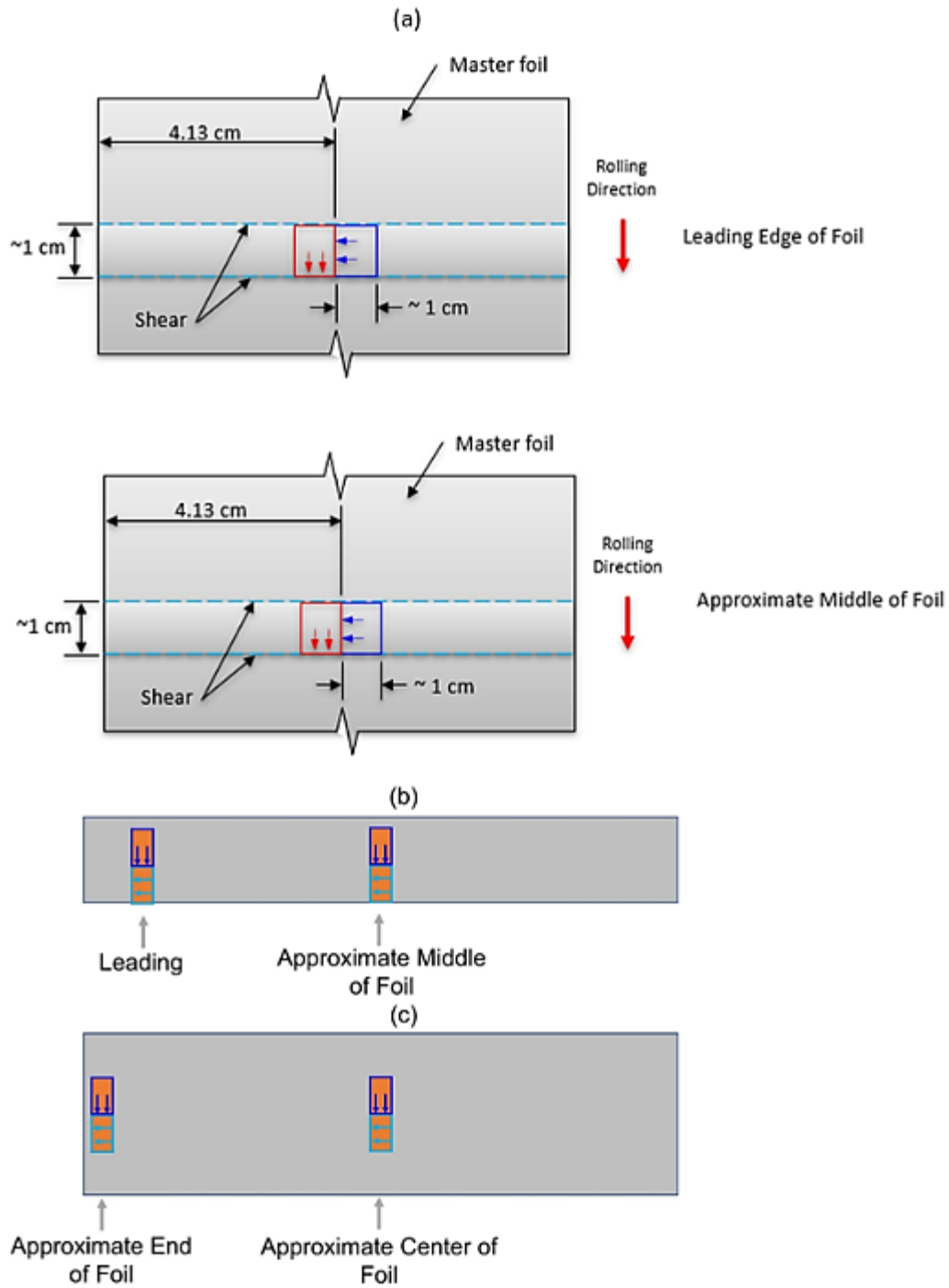


Figure 1. Sectioning diagram according to the Characterization Plan for the Fabrication of U-10Mo Plate Fuel for U.S. High Performance Research Reactors: (a) Master foil, (b) foil and (c) large foil (INL 2021)

## 3.2 Specimen Mounting, Grinding, and Polishing

After sectioning, specimens were mounted using glass slides and epoxy resin for grinding and polishing to expose the fresh specimen surface for observation (optical and scanning electron microscopy [SEM]), and in accordance with the procedure approved by the Characterization Working Group (Prabhakaran et al. 2016). Among the main objectives of a mounting operation are protecting the sample edge and maintaining the integrity of a material's surface features. Mounted specimens (longitudinal and transverse) were polished to a 1,200-grit finish using silicon carbide grinding paper, then further polished using 9  $\mu\text{m}$  and 3  $\mu\text{m}$  diamond suspensions. Final polishing (using a vibratory polisher) was performed using 1  $\mu\text{m}$  diamond suspension and then 0.08  $\mu\text{m}$  colloidal silica suspension. Additional details about specimen mounting, grinding, and polishing can be found in the sample preparation and examination report (Prabhakaran et al. 2016).

## 3.3 Heat Treatment of As-Cast Specimens

As-cast samples shown in Table 7 were homogenized at 900°C for 144 h in argon atmosphere.

## 4.0 Equipment Used for Analysis

### 4.1 Optical Microscope

After the final polishing, the mounted specimens were stored for at least 48 hours before being examined using an optical microscope. Typically, the grains showed up much better in the polarized mode when these samples had been oxidized in air for at least 48 hours.

Optical metallography was performed using an Olympus BX61M optical microscope with a three-axis automated stage and digital charge-coupled device camera. The objectives used for this study have magnifications of 2.5×, 5×, 10×, 20×, and 50×. Good quality images were obtained by using the polarized light filter. A stage micrometer was periodically employed to verify the functioning of the objectives and software.

Olympus Stream Motion software was used to obtain and record individual and montage images. Using the software along with the automated stage enables the user to define top-left and bottom-right corners of the specimen after choosing a particular magnification. Once the border is set, the software automatically calculates the number of individual images required to obtain a montage of the entire specimen. After recording the first image, the automated stage moves slightly to capture the second image at a different location, and this process continues to document the required number of images. Once the individual images are obtained, the software automatically stitches the images to form a single montage image of the entire specimen.

For each specimen, an overview montage image was captured at 2.5× or 5× magnification (based on foil thickness). Additional images at magnifications 10×, 20×, and 50× were captured at two to three locations (left, center, and right) for each specimen. The Olympus Stream Motion software was also used to adjust contrast and other settings to enhance image quality to that suitable for grain size analysis.

U-10Mo specimens subjected to each set of processing conditions were studied at various magnifications to identify the basic microstructural features, including phases present, degree of homogeneity, Zr thickness, and foil thickness.

The grain sizes of U-10Mo specimens were calculated using images obtained from the optical microscope, using ImageJ software. For each specimen, two to three images (20×; left, center, and right; depending upon the specimen size) were used, and approximately 200–250 grains per specimen were used for the measurement of average grain size and standard deviation. For cast samples, 25–50 grains per specimen were used for grain size analysis.

### 4.2 Scanning Electron Microscope

Before performing SEM imaging, the mounted and polished U-10Mo specimens were cleaned using a Fischione plasma cleaner, and then coated with ~10 nm gold in an SPI-Module sputter coater. The gold-coated specimens were again cleaned using the plasma cleaner.

SEM was employed to evaluate the effects of fabrication parameters on U-10Mo. Microstructural and elemental analyses were carried out using a JEOL JSM-7600F SEM equipped with an Oxford Instruments AZtec X-Max 80 mm<sup>2</sup> energy-dispersive x-ray spectroscopy (EDS) detector and INCA Microanalysis Suite software. The JEOL JSM-7600F

system has the following components: (1) in-lens secondary electron imaging detector; (2) Everhart-Thornley detector (lower electron image, LEI); (3) low-angle backscattered electron (LABE) detector; (4) EDS silicon drift detector (SDD); (5) wavelength-dispersive x-ray spectroscopy (WDS) detector; and (6) electron backscatter diffraction (EBSD) detector. The Oxford Instruments AZtec system's components are (1) an X-Max 80 mm<sup>2</sup> SDD detector (Item 4 above); (2) a Wave WDS detector (Item 5 above); (3) an HKL Nordlys EBSD camera (Item 6 above); and (4) AZtec software.

Typical microscope conditions are the following: 30 keV, 15 mm working distance, 110  $\mu\text{m}$  aperture, and beam current of  $\sim 6 \times 10^{-9}$  A or higher. Higher beam currents allow faster EDS data acquisition. On the JSM-7600F, in SEM mode, images are available from the secondary electron imaging, LEI, and LABE detectors, whereas low magnification mode only offers LEI and LABE images. Additional details about the SEM setup can be found in the sample preparation and examination report (Prabhakaran et al. 2016).

SEM was performed to analyze carbides, impurities, Zr thickness, the U-10Mo–Zr interaction layer, phase transformation, chemical banding, phase, homogeneity, and defects. For U-10Mo specimens without Zr, the following images were taken:

- LEI and LABE images of the U-10Mo at 250 $\times$  and 500 $\times$  (left, center, and right)
- LEI and LABE montage image of U-10Mo at 250 $\times$  (center only; covering entire thickness; 8–10 images to create a center-montage image, as shown in Figure 2).

For U-10Mo specimens with Zr, the following images focusing on the Zr layer were taken in addition to those mentioned above: LEI and LABE images at 500 $\times$  (Zr-layer—top center and Zr-layer—bottom center; 10–12 images each to create a montage image of the Zr layer). Other magnifications were used as needed to observe specific features.

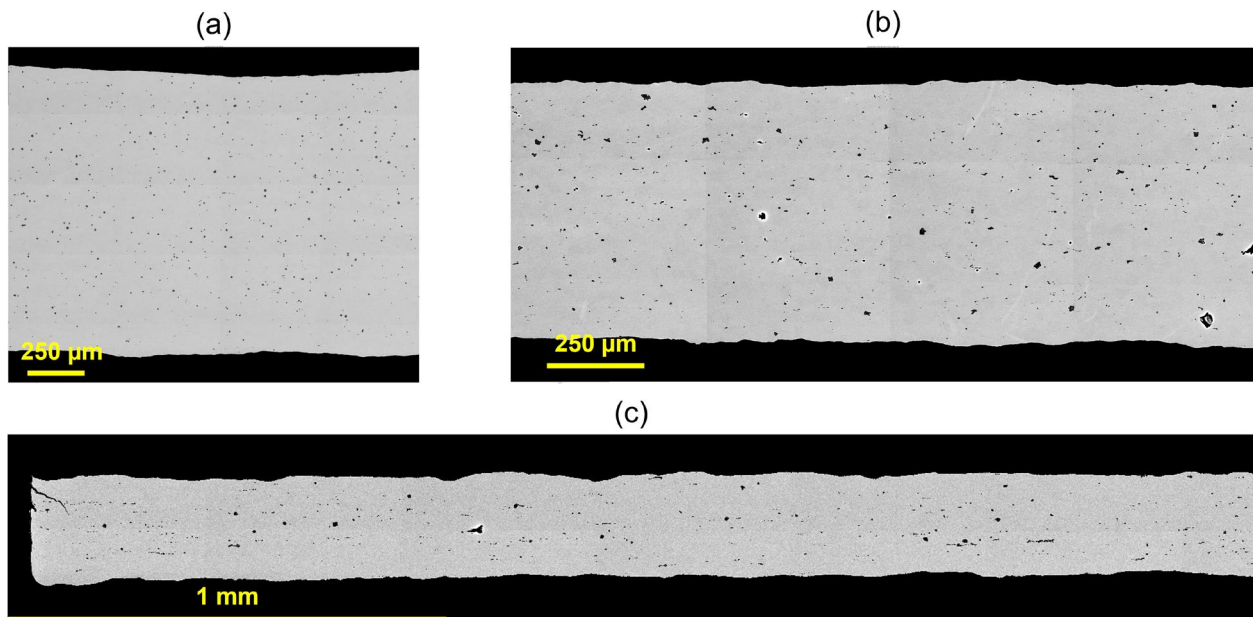


Figure 2. Representative center-montage images of U-10Mo specimens with different thicknesses: (a) LEU-054-03-000-L Long (0.047 in.), (b) LEU-054-01-002-M Long (0.025 in.), and (c) LEU-055-01-001-L Long (0.0105 in.).

Quantitative chemical analysis was performed using EDS. Spectra were collected at a working distance of 15 mm and a voltage of 30 keV. Evaluation of the Mo distribution across the specimen thickness was done in accordance with the MP-2 Characterization Plan (INL 2021): EDS analyses were performed using three line scans (200–300 microns each, depending upon thickness) at the center of the fuel for each specimen at a magnification of 250× and step size of 1 μm. The average of the three line scans for each specimen was used to document Mo weight percent (wt%). During EDS line scanning, x-ray spectra come from the U-10Mo matrix and carbide particles. To avoid including carbide particles in evaluating overall Mo concentration, data points were filtered according to Mo concentration (from 7 to 12 wt%). Data points with values below 7 wt% Mo were ignored because they would be emissions from carbide particles. The carbon concentration in the alloy was not considered during Mo concentration evaluation. Quantitative carbon analysis using EDS is not reliable because carbon has a low atomic number. Finally, the filtered data points were used for estimating average Mo concentration and variation.

### 4.3 Electron Backscatter Diffraction

EBSDF analyses were carried out using a JEOL JSM-7600 field emission SEM, an HKL Nordlys EBSD camera, and an Oxford Instruments NanoAnalysis AZtec Software package. EBSD analyses were performed on a few selected specimens to corroborate the grain size measurements obtained optically. Additional analysis, such as of misorientation and texture, will be performed later.

EBSDF mapping was performed at a working distance of ~24 mm using an accelerating voltage of 20 kV and probe current setting of 16. Camera binning was set to 2 × 2 with a 3.7 Hz acquisition speed and two-frame averaging. Individual maps were recorded at 200× magnification, step sizes ranged from 0.75 μm to 1.25 μm. Indexing of the uranium and uranium carbide (UC) phases was performed using cubic crystal symmetry, and phase details are included in Table 11.

Table 11. EBSD phase details used for phase indexing

Phase	Lattice Parameter	Angles	Space/Laue Group
Gamma Uranium	$a = b = c = 3.41 \text{ \AA}$	$\alpha = \beta = \gamma = 90^\circ$	229/11

Post-processing of the acquired data was performed using the HKL Tango software package by removing extreme spikes and performing an iterative, zero-solution extrapolation to a medium level. Grain size analysis was performed using a 10° critical misorientation to define boundaries. Boundary completion down to 2° was applied in addition to a four-pixel minimum-area grain filter. The carbide phases were excluded from the grain size analysis of the specimen matrix. Border grains located on the edge of the map were included in the grain size determination and weighted according to the number of borders with which any given grain is in contact. (A 2× multiplier is used when a grain is in contact with a single border, whereas a 4× multiplier is used if a single grain is in contact with two borders).

## 5.0 Results and Discussion

This section presents a summary of the results, discussion, and representative images of microstructural features observed in U-10Mo specimens.

### 5.1 Grain Size

#### 5.1.1 Grain Size Measurement Using Optical Microscope

A summary of the grain size results obtained for various U-10Mo specimens, (as-cast, as-cast + homogenized, different foil thicknesses) is presented in Table 12 and Table 13.

Representative microstructures of as-cast and as-cast + homogenized samples used for grain size measurement are shown in Figure 3. Dendritic microstructure was observed in some as-cast samples (Figure 3b), but after homogenization, all specimens had equiaxed microstructure (Figure 3c, d). A summary of grain sizes of cast specimens is given in Table 12. In cast samples, the measured average grain size is in the range of 130–417  $\mu\text{m}$ . After homogenization at 900°C for 144 h, average grain size remains similar; no significant difference in grain sizes before and after homogenization was observed.

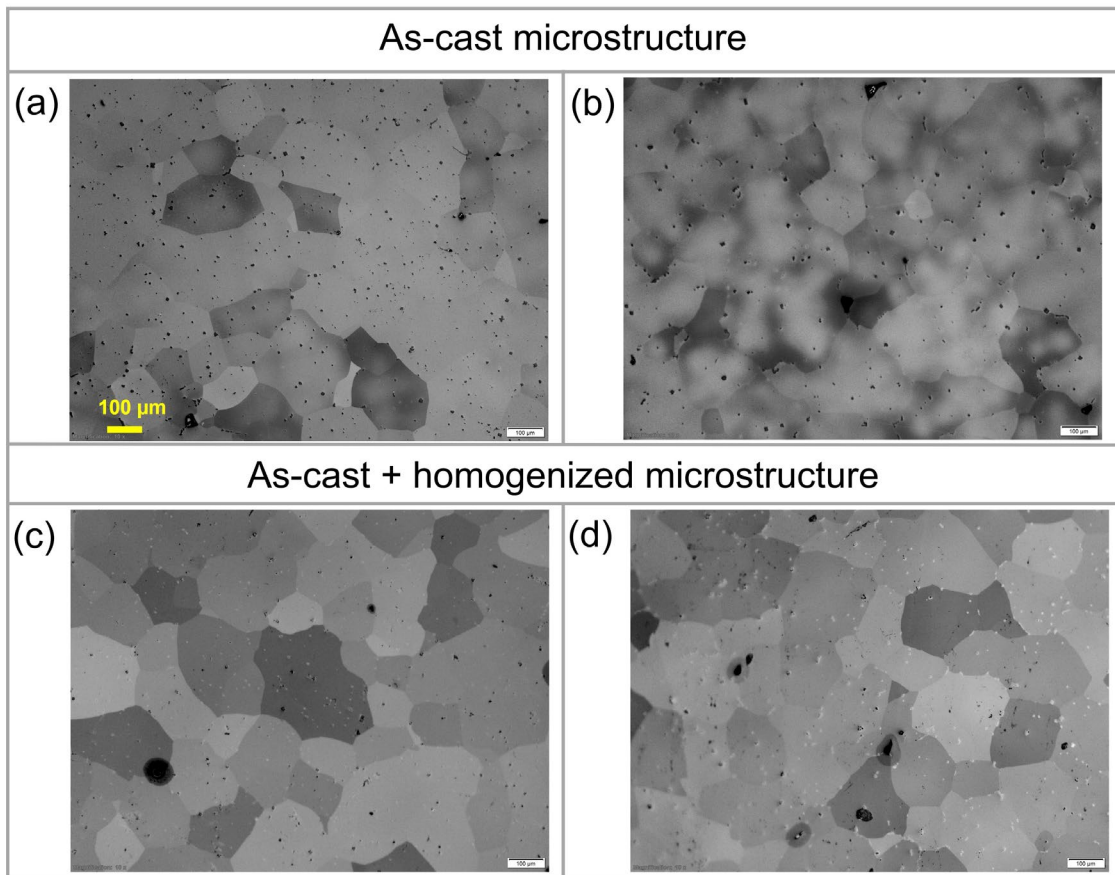


Figure 3. Representative microstructures of cast specimens. As-cast: (a) 3L50-CC-1N14\_1 and (b) 3L50-CC-2N14\_1; as-cast + homogenized: (c) 3L50-CC-1N14\_1 and (d) 3L50-CC-2N14\_1.

Table 12. Grain size of U-10Mo cast and cast + homogenized specimens

Casting	Processing Condition	Sample ID	Met ID	Grain Size ( $\mu\text{m}$ )	SD <sup>(a)</sup> ( $\mu\text{m}$ )
PD-STD2	Cast	3L50-CC-1N14-4	LEU2093	150.5	70.5
	Cast	3L50-CC-1N14-3	LEU2095	160.1	71.7
	Cast	3L50-CC-1N14-1	LEU2094	143.0	70.3
	Cast	3L50-CC-2N14-4	LEU2101	154.5	68.5
	Cast	3L50-CC-2N14-3	LEU2100	169.3	57.3
	Cast	3L50-CC-2N14-1	LEU2099	170.2	70.7
	Cast	3L50-CC-2N15-4	LEU2104	351.5	237.1
	Cast	3L50-CC-2N15-3	LEU2103	416.9	259.5
	Cast	3L50-CC-2N15-1	LEU2102	227.3	150.9
	Cast + homogenized	3L50-CC-1N14-1	LEU2112	154.3	55.4
	Cast + homogenized	3L50-CC-2N14-1	LEU2116	181.3	57.3
	Cast + homogenized	3L50-CC-2N15-1	LEU2117	257.7	170.0

(a) SD = standard deviation

Representative microstructures of specimens with different foil thicknesses used for grain size measurements are shown in Figure 4. Optical microstructure typically displayed fully recrystallized and equiaxed grain structure in master foils and foils (with 0.025 in. and 0.010 in. thick). Very few elongated/ unrecrystallized grains were observed in most of the master foils (0.047 in. thick). Among U-10Mo specimens with different thicknesses, the average grain size decreased as foil thickness decreased. This is the effect of thickness reduction; more thickness reduction introduces more nucleation sites for new recrystallized grains. A summary of grain sizes for all the foils characterized is given in Table 13. The average grain size in master foils (0.047 in. thick) is in the range of 22–32  $\mu\text{m}$ . Average grain sizes for 0.025 in. and 0.010 in. thick foils are in the ranges of 16–21  $\mu\text{m}$  and 14–18  $\mu\text{m}$ , respectively.

Very uniform and recrystallized grain structure was observed in 0.025 in. thick large foils. The average grain size in these foils is in the range of 17–19  $\mu\text{m}$ . However, elongated, deformed microstructure was observed in 0.010 in. thick large foils. Figure 5 shows representative microstructures of 0.025 in. and 0.0105 in. thick large foil samples.

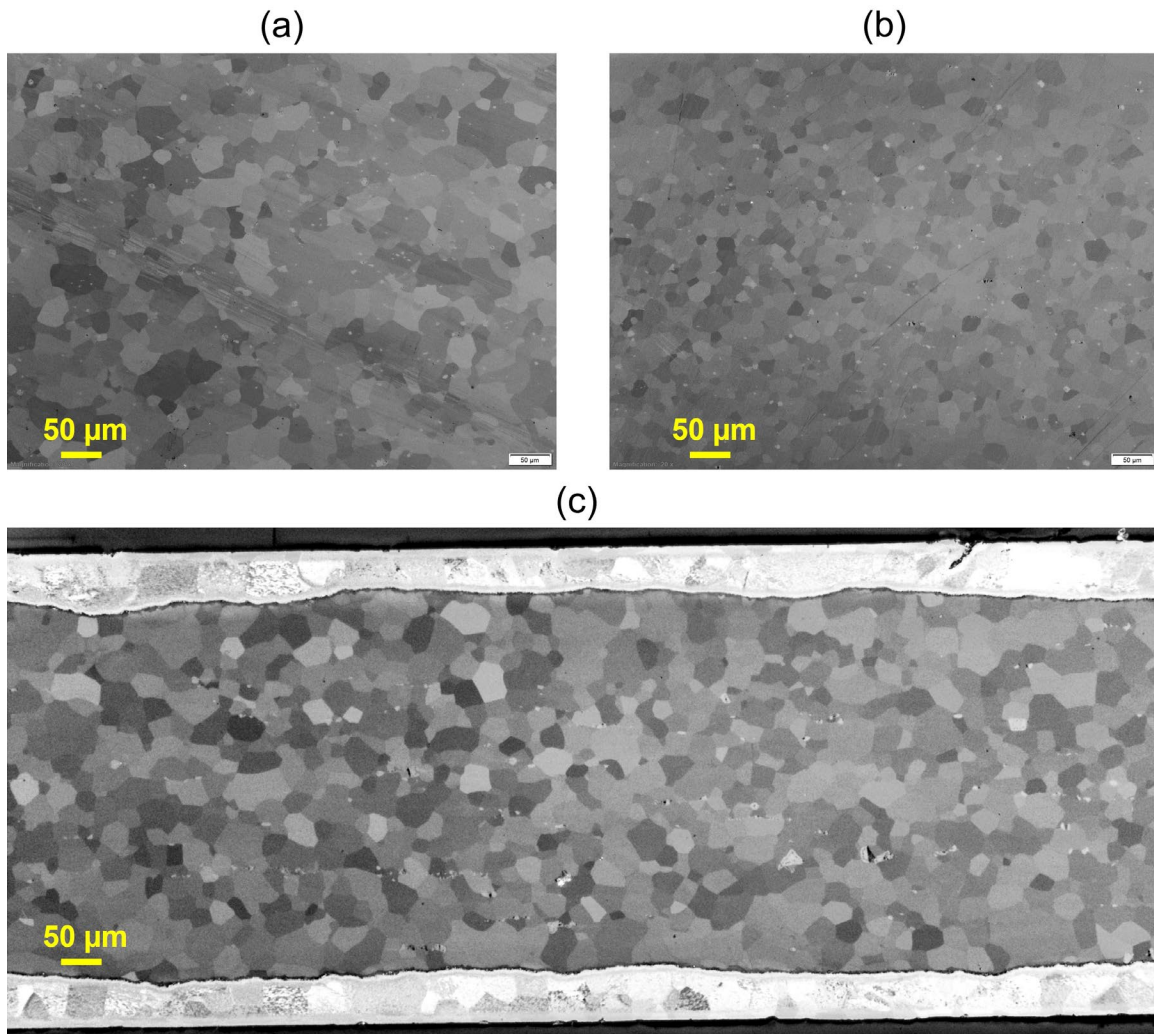


Figure 4. Representative microstructures of foil specimens with different thicknesses: (a) LEU-054-01-000-L Long (0.047 in. thick), (b) LEU-054-01-001-L Long (0.025 in. thick), and (c) LEU-055-01-001-L Long (0.0105 in. thick)

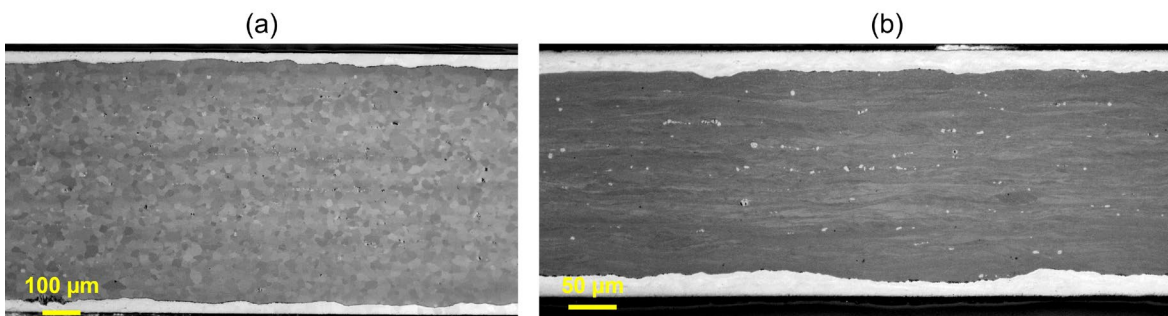


Figure 5. Representative microstructures of plate specimens with different thicknesses: (a) 1MP-20-027-Center Long (0.025 in. thick) and (b) 1MP-20-0105-Center Long (0.0105 in. thick)

Table 13. Grain sizes of U-10Mo specimens obtained by optical microscopy

Thickness (inch)	Processed Condition	Sample ID	Met ID	Direction	Grain Size ( $\mu\text{m}$ )	SD ( $\mu\text{m}$ )
0.047	Master foil	054-01-000 L	LEU2030	Long	28.7	13.5
			LEU2031	Trans	26.2	13.2
0.047	Master foil	054-01-000 M	LEU2032	Long	21.9	9.7
			LEU2033	Trans	32.4	18.8
0.047	Master foil	054-02-000 L	LEU2034	Long	26.9	14.3
			LEU2035	Trans	27.1	12.7
0.047	Master foil	054-02-000 M	LEU2043	Long	25.1	10.2
			LEU2044	Trans	23.6	8.9
0.047	Master foil	054-03-000 L	LEU2047	Long	26.3	10.2
			LEU2048	Trans	25.9	10.0
0.047	Master foil	054-03-000 M	LEU2045	Long	24.8	10.5
			LEU2046	Trans	26.7	9.4
0.047	Master foil	055-01-000 L	LEU2051	Long	24.6	10.4
			LEU2052	Trans	27.5	12.1
0.047	Master foil	055-01-000 M	LEU2053	Long	24.3	11.7
			LEU2055	Trans	29.1	12.6
0.047	Master foil	055-02-000 L	LEU2068	Long	26.4	10.5
			LEU2070	Trans	29.2	13.8
0.047	Master foil	055-02-000 M	LEU2067	Long	27.2	11.4
			LEU2069	Trans	31.4	15.3
0.025	Foil	054-01-001 L	LEU2021	Long	20.9	8.4
			LEU2018	Trans	19.5	7.3
0.025	Foil	054-01-002 M	LEU2024	Long	17.9	6.8
			LEU2025	Trans	17.6	7.0
0.025	Foil	054-02-001 L	LEU2026	Long	18.0	7.1
			LEU2027	Trans	16.4	7.1
0.025	Foil	054-02-002 M	LEU2028	Long	19.1	7.2
			LEU2029	Trans	17.9	7.0
0.025	Foil	054-03-001 L	LEU2022	Long	18.7	7.9
			LEU2019	Trans	17.3	6.6
0.025	Foil	054-03-002 M	LEU2023	Long	18.9	5.9
			LEU2020	Trans	18.7	7.9
0.010	Foil	055-01-001 L	LEU2036	Long	15.0	6.1
			LEU2037	Trans	13.7	5.3
0.010	Foil	055-01-002 M	LEU2049	Long	15.7	5.2
			LEU2050	Trans	16.6	5.4
0.010	Foil	055-02-001 L	LEU2057	Long	15.6	5.5
			LEU2058	Trans	15.7	5.2
0.010	Foil	055-02-001 M	LEU2054	Long	17.3	7.0
			LEU2056	Trans	17.8	7.0

Thickness (inch)	Processed Condition	Sample ID	Met ID	Direction	Grain Size ( $\mu\text{m}$ )	SD ( $\mu\text{m}$ )
0.025	Large foil	1MP-20-027 center	LEU2072	Long	18.0	6.3
			LEU2071	Trans	16.8	5.7
		1MP-20-027 End	LEU2073	Long	19.3	6.8
			LEU2074	Trans	17.4	5.8
0.025	Large foil	2MP-20-027 center	LEU2075	Long	17.6	6.8
			LEU2076	Trans	19.6	6.5
		2MP-20-027 End	LEU2077	Long	18.4	6.5
			LEU2078	Trans	18.5	6.7
0.010	Large foil	1MP-20-0105 center	LEU2083	Long	Deformed	
			LEU2084	Trans	Deformed	
		1MP-20-0105 End	LEU2085	Long	Deformed	
			LEU2086	Trans	Deformed	
0.010	Large foil	2MP-20-0105 center	LEU2079	Long	Deformed	
			LEU2080	Trans	Deformed	
		2MP-20-0105 center	LEU2081	Long	Deformed	
			LEU2082	Trans	Deformed	

### 5.1.2 Grain Size Measurements Using EBSD

Orientation-based imaging was carried out to study the microstructural state (deformed or recrystallized) and perform grain size calculation. This report includes results of recent orientation-based microstructural characterization performed using EBSD on three samples of different thicknesses, 0.047 in. (LEU2051), 0.025 in. (LEU2021) and 0.010 in. (LEU2036). The microstructures of these three specimens are shown in Figure 6. The grains are equiaxed and fully recrystallized. No abnormal grain growth was observed.

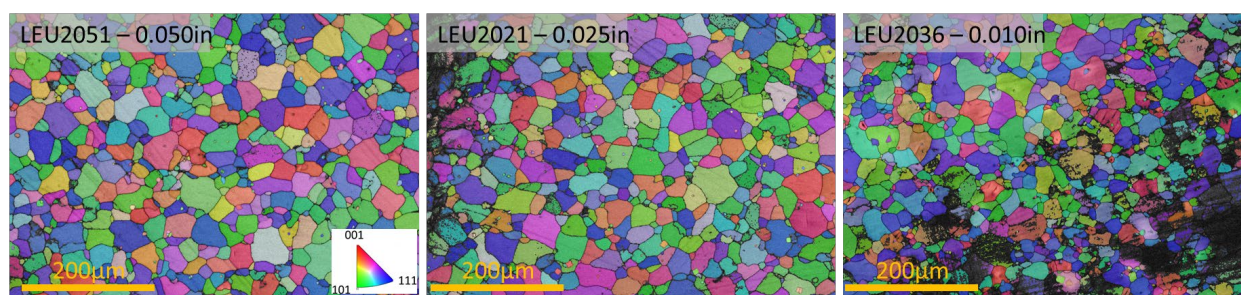


Figure 6. EBSD-generated microstructures of U-10Mo specimens: (a) 055-01--000-L (Long) (0.047 in. thick), (b) 054-01-001-L (Long) (0.025 in. thick) and (c) 055-01-001-L (Long) (0.010 in. thick)

The grain size distributions, in the form of equivalent circle diameters (ECDs), calculated from EBSD microstructures are shown in Figure 7. The total numbers of grains considered for average grain size and grain size distribution are 681, 774, and 1,110 for samples LEU2051, LEU2021, and LEU2036, respectively. Grain sizes measured using EBSD show a slight decrease in value compared to those from optical micrographs (Figure 7). Hand calculations of measurements are prone to human error and can be subject to bias. EBSD uses numerous algorithms to provide the best estimate of the true grain size, which can explain the slight

discrepancy in the grain size results from the two methods. EBSD scans used in this calculation were limited to select sample areas due to sample size limitations and poor diffraction conditions. When the area used for size estimation is limited, the variation in grain sizes throughout the sample may not be captured completely in EBSD; optical microscopy is not affected as much by surface damage or diffraction capability. Thus, optical microscopy is able to capture a larger area faster than EBSD can in this case. However, overall trend in variation of grain size with thickness reduction remains same in both the measurement methods.

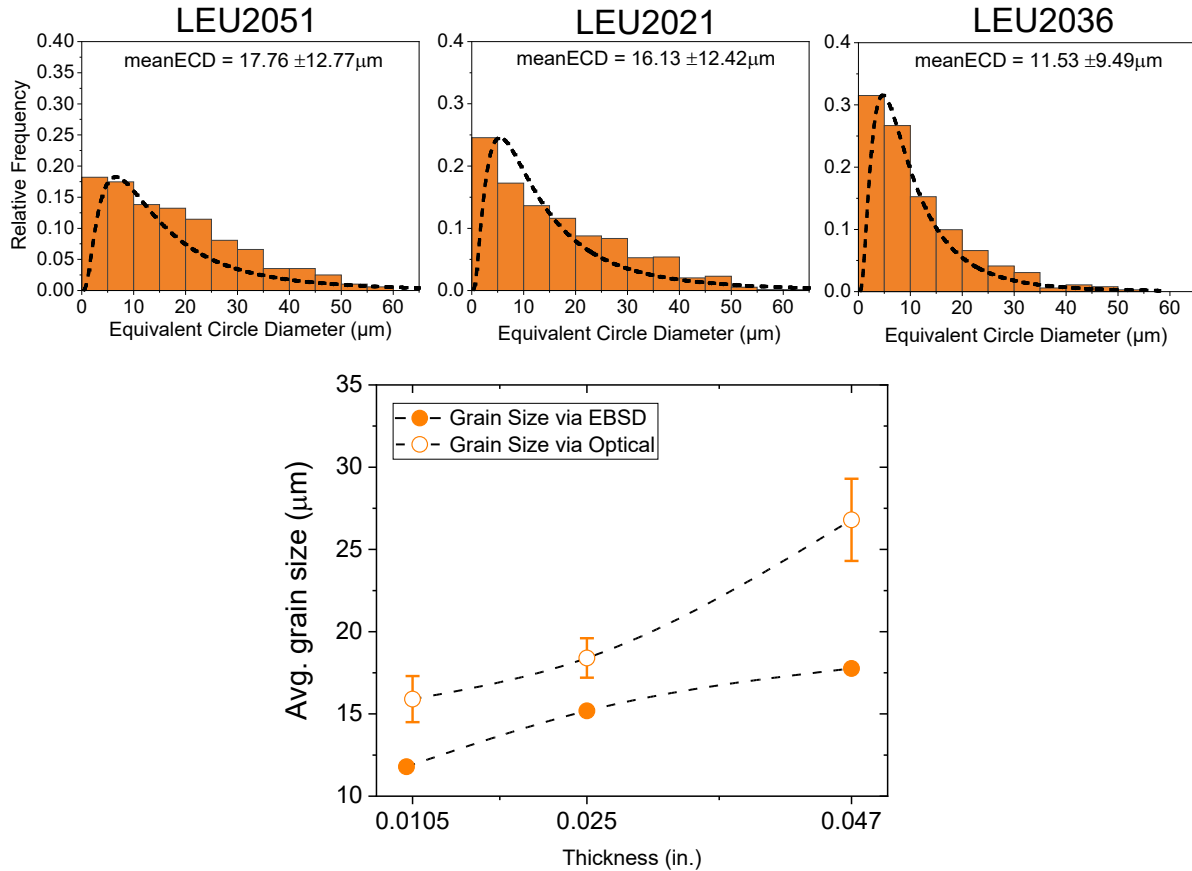


Figure 7. Grain size distribution calculated from EBSD microstructures for LEU2051, LEU2021, and LEU2036 (0.047 in., 0.025 in., and 0.010 in. thick, respectively). When the thickness is smaller, more smaller grains can be seen, which reduces the mean grain size.

## 5.2 Molybdenum Distribution and Chemical Banding

The U-10Mo as-cast microstructure is an inhomogeneous, dendritic structure with Mo-rich and Mo-lean regions (Nyberg et al. 2013; Nyberg et al. 2014; Joshi et al. 2015). Mo segregation during the casting process is detrimental because it may affect the  $\gamma$ -phase stability, and it could lead to formation of an  $\alpha$  phase, and to the phase transition from  $\gamma$  to  $\alpha + \gamma'$  during thermal annealing (Jana et al. 2017).

A homogenization process is needed to reduce Mo segregation and produce the desired microstructure with uniformly distributed Mo. Homogenization of U-10Mo is performed in the

$\gamma$ -phase field (above 560°C) for 48–144 hours, depending upon the temperature (Burkes et al. 2010; Nyberg et al. 2014; Joshi et al. 2015; Bostrom and Halteman 1956). Experiments were performed earlier to determine the optimum homogenization temperature and time for the U-10Mo alloy. All the samples were homogenized (at 900°C for 144 hours) prior to thermomechanical processing for the MP-2 experiment.

Quantitative chemical analysis was performed using EDS analyses. The EDS analyses were performed on each specimen to evaluate the Mo distribution across the specimen thickness. In cast samples, EDS was performed at three locations: left, center, and right side of the specimen. In each location, measurements were done across the two lines with 300 data points per line. A representative Mo distribution (from a line scan across the specimen thickness) is shown in Figure 8 for a U-10Mo specimen, LEU-054-01-000-L Long (0.047 in. thick). The Mo distribution obtained from the EDS line analyses for cast specimens, foils, and large foils of U-10Mo are shown in Table 14 and Table 15. The tables show average Mo concentration and standard deviation (SD) of Mo content in the specimens. While calculating the Mo concentration, efforts were made to avoid UC regions.<sup>1</sup>

In as-cast samples, the standard deviation of Mo content is more than 0.5 wt% in the majority of samples (Table 14). However, after homogenization, Mo variation is below 0.5 wt%, which indicates specimens met Mo concentration specification. Compositions measured at Y-12 after casting using inductively coupled plasma mass spectrometry (ICP-MS) are also shown in Table 14. Measurements were performed at six locations for each cast sample. The average Mo content is about 10 wt% with SD less than 0.5 wt%.

---

<sup>1</sup> PNNL-27814, Pacific Northwest National Laboratory, Richland, WA. (Limited distribution)

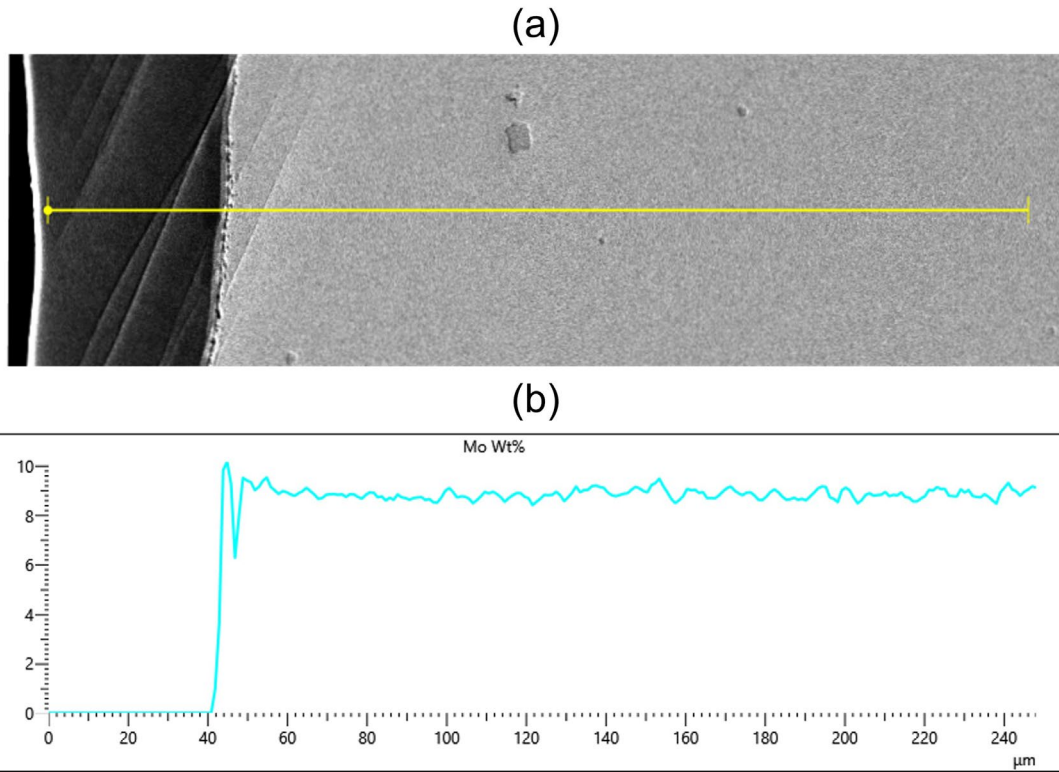


Figure 8. Mo distribution (along a line scan across the specimen thickness) for a U-10Mo specimen of thickness 0.047 in. (LEU-054-01-000-L Long)

Table 14. Mo distribution (EDS measurements) in U-10Mo as-cast and as-cast + homogenized specimens

Casting	Processed Condition	Sample ID	Met ID	Mo (wt%)	SD (wt%)	Points #	Y-12 Mo (wt%)	SD (wt%)
PD-STD2	Cast	3L50-CC-1N14-4	LEU2093	9.2	0.47	1800	10.4	0.40
	Cast	3L50-CC-1N14-3	LEU2095	9.8	0.70	1800		
	Cast	3L50-CC-1N14-1	LEU2094	8.8	0.45	1796		
	Cast	3L50-CC-2N14-4	LEU2101	9.8	0.51	1800	10.4	0.33
	Cast	3L50-CC-2N14-3	LEU2100	9.8	0.60	1800		
	Cast	3L50-CC-2N14-1	LEU2099	9.4	0.49	1800		
	Cast	3L50-CC-2N15-4	LEU2104	9.5	0.51	1800	10.3	0.35
	Cast	3L50-CC-2N15-3	LEU2103	9.4	0.65	1797		
	Cast	3L50-CC-2N15-1	LEU2102	9.5	0.39	1800		
	Cast + homogenized	3L50-CC-1N14-1	LEU2112	8.9	0.30	1800	N/A	N/A
	Cast + homogenized	3L50-CC-2N14-1	LEU2116	9.8	0.26	1800		
Cast + homogenized	3L50-CC-2N15-1	LEU2117	9.2	0.30	1800			

In foil specimens, the average Mo content was about 9.5 wt% in most of the specimens, with a standard deviation of less than 0.5% for all specimens. All foil specimens showed nearly homogeneous Mo distribution and no chemical banding was observed. EDS analysis was performed at left, center, and right of each specimen across three lines. The Mo distribution obtained from the EDS line analyses for foils and large-foil U-10Mo specimens are shown in Table 15. In case of plates (with 0.025 in. and 0.010 in. thickness), Mo distribution is very homogeneous with deviation less than 0.5 %. Here also, UC particles were ignored in calculating Mo content.

Table 15. Mo distribution (EDS measurements) in U-10Mo foil specimens

Thickness (inch)	Processed Condition	Sample ID	Met ID	Direction	Mo (wt%)	SD	#Points	Banding
0.047	Master foil	054-01-000 L	LEU2030	Long	9.4	0.33	724	No
			LEU2031	Trans	8.9	0.34	724	No
0.047	Master foil	054-01-000 M	LEU2032	Long	9.5	0.31	729	No
			LEU2033	Trans	9.5	0.27	726	No
0.047	Master foil	054-02-000 L	LEU2034	Long	9.4	0.37	725	No
			LEU2035	Trans	9.4	0.31	731	No
0.047	Master foil	054-02-000 M	LEU2043	Long	9.6	0.35	728	No
			LEU2044	Trans	9.5	0.44	730	No
0.047	Master foil	054-03-000 L	LEU2047	Long	9.4	0.30	590	No
			LEU2048	Trans	9.5	0.30	607	No
0.047	Master foil	054-03-000 M	LEU2045	Long	9.4	0.39	722	No
			LEU2046	Trans	9.6	0.34	579	No
0.047	Master foil	055-01-000 L	LEU2051	Long	9.6	0.36	737	No
			LEU2052	Trans	9.6	0.32	732	No
0.047	Master foil	055-01-000 M	LEU2053	Long	9.6	0.36	737	No
			LEU2055	Trans	9.5	0.32	728	No
0.047	Master foil	055-02-000 L	LEU2068	Long	9.4	0.30	730	No
			LEU2070	Trans	9.3	0.31	722	No
0.047	Master foil	055-02-000 M	LEU2067	Long	9.0	0.28	727	No
			LEU2069	Trans	8.1	0.28	720	No
0.025	Foil	054-01-001 L	LEU2021	Long	9.0	0.34	665	No
			LEU2018	Trans	9.0	0.40	653	No
0.025	Foil	054-01-002 M	LEU2024	Long	9.6	0.29	669	No
			LEU2025	Trans	9.6	0.33	672	No
0.025	Foil	054-02-001 L	LEU2026	Long	9.8	0.34	671	No
			LEU2027	Trans	9.6	0.42	684	No
0.025	Foil	054-02-002 M	LEU2028	Long	9.1	0.34	672	No
			LEU2029	Trans	9.2	0.37	687	No
0.025	Foil	054-03-001 L	LEU2022	Long	9.5	0.28	671	No
			LEU2019	Trans	9.5	0.31	681	No
0.025	Foil	054-03-002 M	LEU2023	Long	9.7	0.30	656	No
			LEU2020	Trans	9.6	0.35	652	No

Thickness (inch)	Processed Condition	Sample ID	Met ID	Direction	Mo (wt%)	SD	#Points	Banding
0.010	Foil	055-01-001 L	LEU2036	Long	9.6	0.32	648	No
			LEU2037	Trans	9.6	0.25	672	No
0.010	Foil	055-01-002 M	LEU2049	Long	9.6	0.64	623	No
			LEU2050	Trans	9.5	0.39	587	No
0.010	Foil	055-02-001 L	LEU2057	Long	9.3	0.34	656	No
			LEU2058	Trans	9.4	0.35	655	No
0.010	Foil	055-02-001 M	LEU2054	Long	8.6	0.36	626	No
			LEU2056	Trans	8.7	0.28	627	No
0.025	Large foil	1MP-20-027 center	LEU2072	Long	9.7	0.38	650	No
			LEU2071	Trans	9.7	0.33	659	No
0.025	Large foil	1MP-20-027 End	LEU2073	Long	9.7	0.29	670	No
			LEU2074	Trans	9.6	0.38	661	No
0.025	Large foil	2MP-20-027 Center	LEU2075	Long	9.1	0.27	732	No
			LEU2076	Trans	9.1	0.25	731	No
0.025	Large foil	2MP-20-027 End	LEU2077	Long	9.1	0.32	723	No
			LEU2078	Trans	9.1	0.30	734	No
0.010	Large foil	1MP-20-0105 center	LEU2083	Long	9.3	0.29	662	No
			LEU2084	Trans	9.4	0.32	667	No
0.010	Large foil	1MP-20-0105 End	LEU2085	Long	9.4	0.30	635	No
			LEU2086	Trans	9.3	0.33	659	No
0.010	Large foil	2MP-20-0105 center	LEU2079	Long	9.3	0.31	649	No
			LEU2080	Trans	9.4	0.25	641	No
0.010	Large foil	2MP-20-0105 End	LEU2081	Long	9.3	0.31	653	No
			LEU2082	Trans	9.3	0.31	674	No

### 5.3 Carbide Fraction and Size Evaluation

Carbide volume fraction and size analysis were performed because they have a strong influence on microstructure and foil fabrication. Carbides are easily identified based upon their darker contrast with respect to the matrix while using a backscattered electron (BSE) detector, as shown in Figure 9. The carbide area fraction in U-10Mo specimens was evaluated using SEM images obtained with a BSE detector at 250× magnification. A montage image (area approximately 2,000 μm × 200 μm) consisting of 8–10 individual images at 250× magnification covering the entire fuel thickness at the specimen center was used to improve statistics (as compared to a single image). The carbide particle size/area analysis was performed using 3–5 individual SEM images (at different locations) obtained with a BSE detector at 250× magnification.

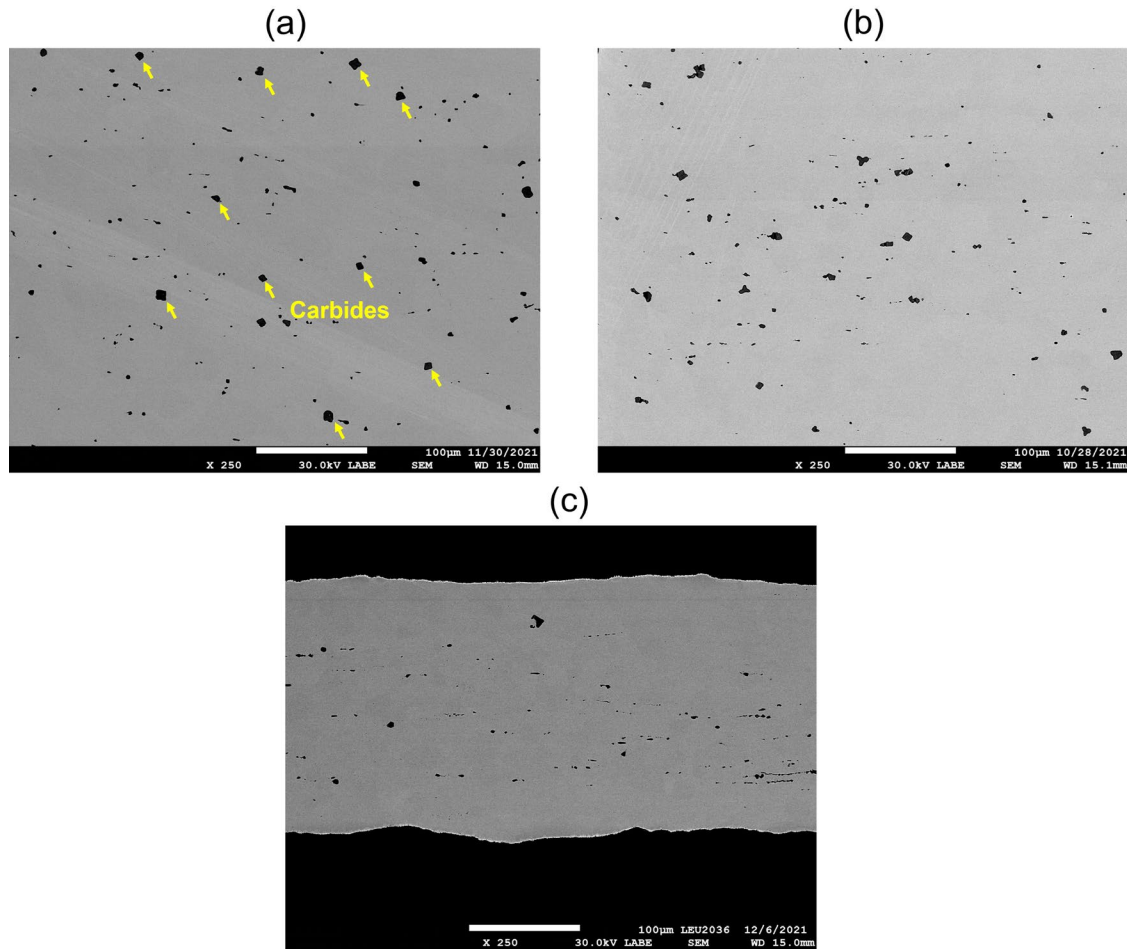


Figure 9. BSE-SEM microstructures of U-10Mo specimens of thickness 0.01 in.:  
 (a) LEU-054-01-000-L Long (0.047 in.), (b) LEU-054-01-001-L Long (0.025 in.), and  
 (c) LEU-055-01-001-L Long (0.0105 in.)

ImageJ software was employed for calculating area fraction and for particle area analysis. A sequential procedure for the ImageJ analysis method is given in Figure 10. A thresholding method was used for distinguishing carbide particles from the matrix. Representative microstructures after ImageJ thresholding are shown in Figure 11. ImageJ-threshold images were used for the calculation of carbide area fractions and their distributions.

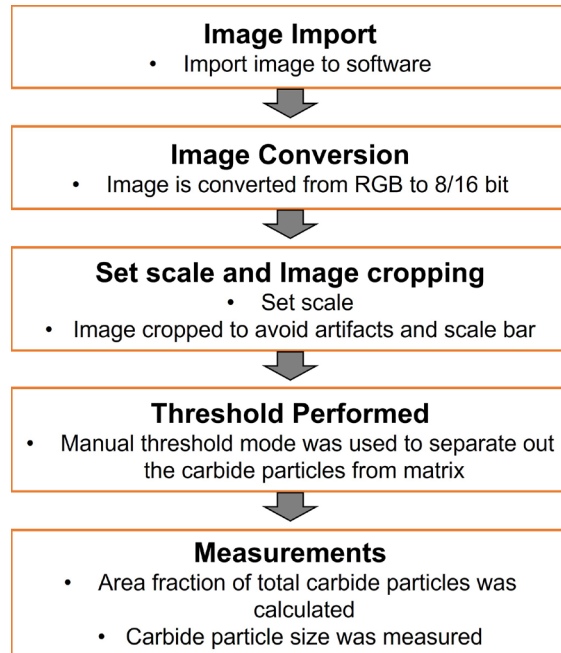


Figure 10. Schematic illustration of steps performed while using ImageJ analysis software

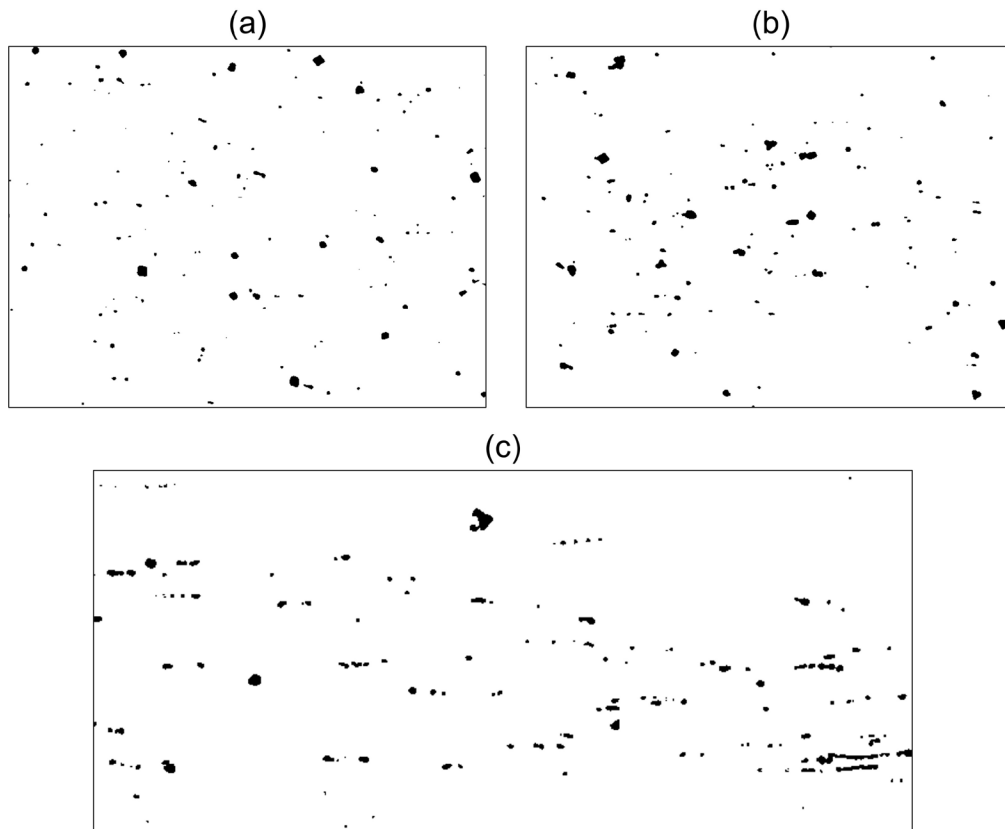


Figure 11. BSE-SEM microstructures of U-10Mo specimens of thickness 0.01 in. after ImageJ thresholding: (a) LEU-054-01-000-L Long (0.047 in.), (b) LEU-054-01-001-L Long (0.025 in.), and (c) LEU-055-01-001-L Long (0.0105 in.)

The thickness reduction during rolling reduction passes and the annealing processes will redistribute the carbides, during which they tend to form stringers (Cheng et al. 2018; Hu et al. 2018). Carbide stringers of a typical length of 10 to 70  $\mu\text{m}$  were observed in U-10Mo specimens. A summary of carbide area fractions in cast and foil U-10Mo specimens, is provided in Table 16 and Table 17. Almost all the as-cast and as-cast + homogenized specimens showed carbide fractions less than 1.5%. Similarly, carbide area fraction analysis was performed on foils and plate specimens and showed carbide content less than 1.0%. Any submicron- and nanometer-size particles present in the microstructure that were not resolved by SEM might have been excluded from the area fraction calculation by the software. Figure 12a shows a box plot of average carbide fraction for as-cast and foil specimens. Carbon content (ppm) is calculated from the carbide fractions is also given in Table 16 and Table 17.

**Table 16. Carbide area fraction in cast and cast + homogenized U-10Mo specimens**

Casting	Processed Condition	Sample ID	Met ID	Carbide (%)	SD	C (ppm)
PD-STD2	Cast	3L50-CC-1N14-4	LEU2093	1.1	0.10	421
	Cast	3L50-CC-1N14-3	LEU2095	1.4	0.05	536
	Cast	3L50-CC-1N14-1	LEU2094	1.1	0.04	421
	Cast	3L50-CC-2N14-4	LEU2101	0.98	0.05	375
	Cast	3L50-CC-2N14-3	LEU2100	1.3	0.08	498
	Cast	3L50-CC-2N14-1	LEU2099	1.2	0.07	460
	Cast	3L50-CC-2N15-4	LEU2104	1.4	0.19	536
	Cast	3L50-CC-2N15-3	LEU2103	1.3	0.10	498
	Cast	3L50-CC-2N15-1	LEU2102	1.3	0.21	498
	Cast + homogenized	3L50-CC-1N14-1	LEU2112	0.73	0.22	280
	Cast + homogenized	3L50-CC-2N14-1	LEU2116	1.2	0.07	460
	Cast + homogenized	3L50-CC-2N15-1	LEU2117	1.3	0.07	498

**Table 17. Carbide area fraction in U-10Mo foil specimens**

Thickness (inch)	Processed Condition	Sample ID	Met ID	Direction	Carbide (%)	SD	C (ppm)
0.047	Master foil	054-01-000 L	LEU2030	Long	0.88	0.10	337
			LEU2031	Trans	0.64	0.12	245
0.047	Master foil	054-01-000 M	LEU2032	Long	0.84	0.04	322
			LEU2033	Trans	0.84	0.17	322
0.047	Master foil	054-02-000 L	LEU2034	Long	0.90	0.26	345
			LEU2035	Trans	0.73	0.16	280
0.047	Master foil	054-02-000 M	LEU2043	Long	0.97	0.05	372
			LEU2044	Trans	0.90	0.16	345
0.047	Master foil	054-03-000 L	LEU2047	Long	0.83	0.13	318
			LEU2048	Trans	0.85	0.10	326
0.047	Master foil	054-03-000 M	LEU2045	Long	0.99	0.11	379

Thickness (inch)	Processed Condition	Sample ID	Met ID	Direction	Carbide (%)	SD	C (ppm)
0.047	Master foil	055-01-000 L	LEU2046	Trans	0.91	0.02	349
			LEU2051	Long	0.82	0.19	314
			LEU2052	Trans	0.69	0.05	264
0.047	Master foil	055-01-000 M	LEU2053	Long	0.80	0.10	307
			LEU2055	Trans	0.89	0.07	341
0.047	Master foil	055-02-000 L	LEU2068	Long	0.88	0.07	337
			LEU2070	Trans	0.88	0.13	337
0.047	Master foil	055-02-000 M	LEU2067	Long	0.92	0.04	352
			LEU2069	Trans	0.96	0.05	368
0.025	Foil	054-01-001 L	LEU2021	Long	0.80	0.10	307
			LEU2018	Trans	0.63	0.10	241
0.025	Foil	054-01-002 M	LEU2024	Long	0.96	0.24	368
			LEU2025	Trans	0.96	0.04	368
0.025	Foil	054-02-001 L	LEU2026	Long	1.1	0.14	421
			LEU2027	Trans	1.1	0.13	421
0.025	Foil	054-02-002 M	LEU2028	Long	0.93	0.17	356
			LEU2029	Trans	0.83	0.02	318
0.025	Foil	054-03-001 L	LEU2022	Long	0.76	0.25	291
			LEU2019	Trans	0.86	0.06	330
0.025	Foil	054-03-002 M	LEU2023	Long	1.01	0.07	387
			LEU2020	Trans	1.0	0.10	383
0.010	Foil	055-01-001 L	LEU2036	Long	0.90	0.16	345
			LEU2037	Trans	0.94	0.06	360
0.010	Foil	055-01-002 M	LEU2049	Long	0.96	0.16	368
			LEU2050	Trans	0.93	0.10	356
0.010	Foil	055-02-001 L	LEU2057	Long	1.05	0.10	402
			LEU2058	Trans	0.94	0.10	360
0.010	Foil	055-02-001 M	LEU2054	Long	0.81	0.10	310
			LEU2056	Trans	0.94	0.07	360
0.025	Large foil	1MP-20-027 center	LEU2072	Long	0.94	0.18	360
			LEU2071	Trans	0.88	0.06	337
			LEU2073	Long	1.04	0.22	398
0.025	Large foil	1MP-20-027 End	LEU2074	Trans	0.92	0.13	352
			LEU2075	Long	0.80	0.05	307
			LEU2076	Trans	0.90	0.04	345
			LEU2077	Long	0.85	0.06	326
0.025	Large foil	2MP-20-027 center	LEU2078	Trans	0.76	0.11	291
			LEU2083	Long	0.83	0.08	318
			LEU2084	Trans	1.3	0.24	498
0.010	Large foil	1MP-20-0105 center	LEU2085	Long	0.90	0.04	345
			LEU2086	Trans	0.95	0.11	364
0.010	Large foil	2MP-20-0105 center	LEU2079	Long	0.90	0.13	345
			LEU2080	Trans	1.05	0.10	402

Thickness (inch)	Processed Condition	Sample ID	Met ID	Direction	Carbide (%)	SD	C (ppm)
		2MP-20-0105	LEU2081	Long	0.94	0.25	360
		center	LEU2082	Trans	0.91	0.23	349

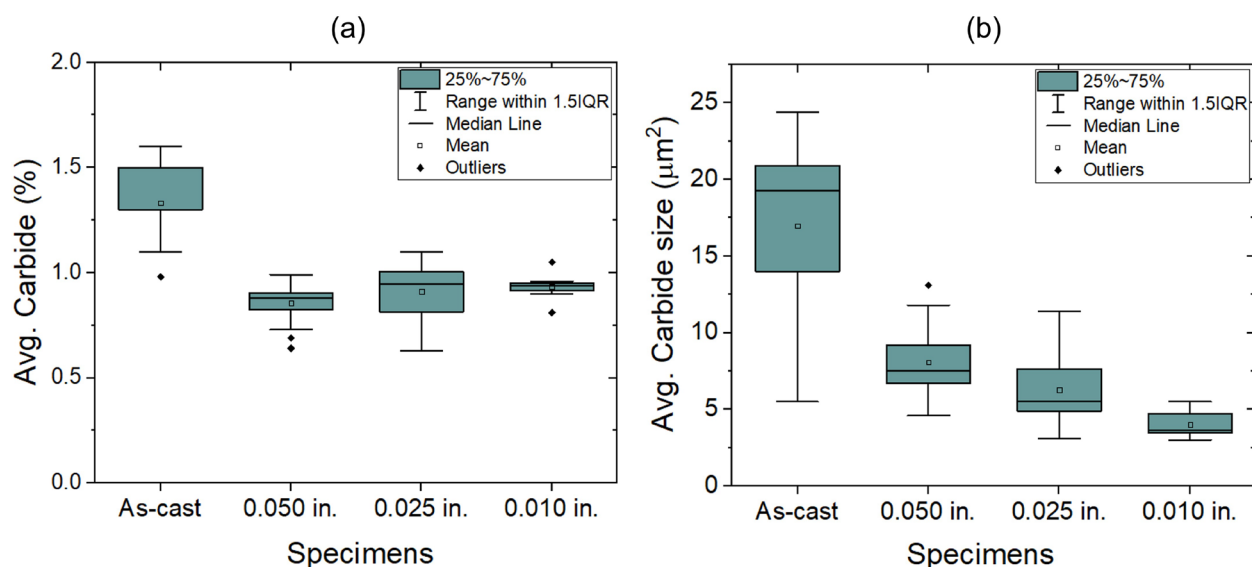


Figure 12. Summary plots of carbide analysis for as-cast and foil samples: (a) volume fraction of carbides and (b) size of carbides

Summaries of the carbide particle size ( $\mu\text{m}^2$ ) in cast and foil U-10Mo specimens are provided in Table 18 and Table , respectively. In as-cast samples, average carbide sizes were in the range of 11–25  $\mu\text{m}^2$ . Carbide size remained almost the same after homogenization as before.

Somewhat lower carbide sizes were observed in foils. Average carbide size for 0.047 in., 0.025 in., and 0.010 in. thick foils are in the ranges of 5–13  $\mu\text{m}^2$ , 3–11  $\mu\text{m}^2$  and 3–5  $\mu\text{m}^2$ , respectively. Figure 12b shows the box plot of average carbide particle size for as-cast and foil specimens. A significant refinement of carbide particles was observed in rolled samples, where carbide size was decreased with thickness reductions.

Average carbide sizes for 0.025 in. and 0.010 in. large foils were in the range of 5–15  $\mu\text{m}^2$  and 3–5  $\mu\text{m}^2$ , respectively.

Table 18. Carbide particle size in U-Mo cast and cast + homogenized specimens

Casting	Processed Condition	Sample ID	Met ID	Avg. Carbide Size ( $\mu\text{m}^2$ )	SD	Min/Max ( $\mu\text{m}^2$ )
	Cast	3L50-CC-1N14-4	LEU2093	11.4	18.2	0.21/212.2
PD-STD2	Cast	3L50-CC-1N14-3	LEU2095	16.6	29.9	0.21/259.3
	Cast	3L50-CC-1N14-1	LEU2094	14.1	32.3	0.21/516.1
	Cast	3L50-CC-2N14-4	LEU2101	19.7	19.9	0.21/106.1

Casting	Processed Condition	Sample ID	Met ID	Avg. Carbide Size ( $\mu\text{m}^2$ )	SD	Min/Max ( $\mu\text{m}^2$ )
	Cast	3L50-CC-2N14-3	LEU2100	20.7	30.8	0.21/190.2
	Cast	3L50-CC-2N14-1	LEU2099	24.4	31.3	0.21/222.4
	Cast	3L50-CC-2N15-4	LEU2104	21.7	22.8	0.24/156.6
	Cast	3L50-CC-2N15-3	LEU2103	20.0	28.1	0.21/286.3
	Cast	3L50-CC-2N15-1	LEU2102	22.6	32.9	0.21/483.5
	Cast + homogenized	3L50-CC-1N14-1	LEU2112	13.4	17.9	0.21/139.8
	Cast + homogenized	3L50-CC-2N14-1	LEU2116	23.6	31.2	0.21/263.2
	Cast + homogenized	3L50-CC-2N15-1	LEU2117	19.2	24.9	0.21/178.8

Table 19. Carbide particle size in U-Mo foil specimens

Thickness (inch)	Processed Condition	Sample ID	Met ID	Direction	Avg. Carbide Size ( $\mu\text{m}^2$ )	SD	Min/Max ( $\mu\text{m}^2$ )
0.047	Master foil	054-01-000 L	LEU2030	Long	7.4	13.6	0.211/131.9
			LEU2031	Trans	6.6	14.1	0.211/213.3
0.047	Master foil	054-01-000 M	LEU2032	Long	6.6	17.2	0.21/193.8
			LEU2033	Trans	10.3	16.1	0.21/144.3
0.047	Master foil	054-02-000 L	LEU2034	Long	8.3	22.5	0.211/173.2
			LEU2035	Trans	8.2	24.3	0.21/241.8
0.047	Master foil	054-02-000 M	LEU2043	Long	4.6	18.0	0.211/268.1
			LEU2044	Trans	9.5	21.8	0.211/184.8
0.047	Master foil	054-03-000 L	LEU2047	Long	6.0	15.5	0.21/168.7
			LEU2048	Trans	7.6	16.6	0.211/114.4
0.047	Master foil	054-03-000 M	LEU2045	Long	6.8	26.9	0.211/382.4
			LEU2046	Trans	10.3	22.6	0.21/163.8
0.047	Master foil	055-01-000 L	LEU2051	Long	7.5	14.4	0.21/180.5
			LEU2052	Trans	7.0	12.6	0.21/115.0
0.047	Master foil	055-01-000 M	LEU2053	Long	13.1	23	0.21/150.3
			LEU2055	Trans	7.5	16.8	0.21/160.5
0.047	Master foil	055-02-000 L	LEU2068	Long	11.8	14.0	0.21/99.7
			LEU2070	Trans	8.9	11.5	0.211/91.1
0.047	Master foil	055-02-000 M	LEU2067	Long	6.6	16.9	0.211/177.8
			LEU2069	Trans	6.9	16.8	0.21/269.9
0.025	Foil	054-01-001 L	LEU2021	Long	5.0	10.7	0.21/109.8
			LEU2018	Trans	4.8	9.0	0.211/77.2
0.025	Foil	054-01-002 M	LEU2024	Long	7.1	16.8	0.211/196.0
			LEU2025	Trans	5.1	13.7	0.21/176.5

Thickness (inch)	Processed Condition	Sample ID	Met ID	Direction	Avg. Carbide Size ( $\mu\text{m}^2$ )	SD	Min/Max ( $\mu\text{m}^2$ )
0.025	Foil	054-02-001 L	LEU2026	Long	8.2	28.9	0.211/275.3
			LEU2027	Trans	5.6	18.5	0.211/201.3
0.025	Foil	054-02-002 M	LEU2028	Long	4.0	12.7	0.211/136.2
			LEU2029	Trans	3.1	10.2	0.211/112.6
0.025	Foil	054-03-001 L	LEU2022	Long	11.4	20.8	0.211/128.0
			LEU2019	Trans	6.9	18.3	0.211/249.2
0.025	Foil	054-03-002 M	LEU2023	Long	5.5	19.2	0.21/222.1
			LEU2020	Trans	8.5	19.1	0.211/123.8
0.010	Foil	055-01-001 L	LEU2036	Long	3.0	8.3	0.211/111.7
			LEU2037	Trans	3.6	8.8	0.211/105.8
0.010	Foil	055-01-002 M	LEU2049	Long	3.5	10.0	0.21/122.8
			LEU2050	Trans	3.5	8.0	0.211/76.2
0.010	Foil	055-02-001 L	LEU2057	Long	3.7	8.5	0.211/89.3
			LEU2058	Trans	4.7	8.3	0.21/73.4
0.010	Foil	055-02-001 M	LEU2054	Long	5.5	10.5	0.21/82.6
			LEU2056	Trans	4.7	10.3	0.211/109.5
0.025	Large foil	1MP-20-027 Center	LEU2072	Long	5.0	18.4	0.211/220.0
			LEU2071	Trans	6.9	18.9	0.21/214.0
0.025	Large foil	1MP-20-027 End	LEU2073	Long	14.7	31.9	0.21/276.7
			LEU2074	Trans	7.2	20.8	0.21/163.1
0.025	Large foil	2MP-20-027 Center	LEU2075	Long	12.0	19.1	0.211/91.6
			LEU2076	Trans	7.5	17.6	0.211/251.7
0.025	Large foil	2MP-20-027 End	LEU2077	Long	11.3	21.5	0.21/167.4
			LEU2078	Trans	4.2	12.1	0.211/112.2
0.010	Large foil	1MP-20-0105 Center	LEU2083	Long	5.4	10.1	0.21/145.6
			LEU2084	Trans	4.4	6.8	0.211/55.5
0.010	Large foil	1MP-20-0105 End	LEU2085	Long	4.8	7.2	0.21/71.9
			LEU2086	Trans	5.6	9.8	0.211/125.7
0.010	Large foil	2MP-20-0105 Center	LEU2079	Long	4.2	8.3	0.21/93.4
			LEU2080	Trans	2.8	6.0	0.21/63.9
0.010	Large foil	2MP-20-0105 End	LEU2081	Long	4.7	9.5	0.21/99.0
			LEU2082	Trans	4.5	6.5	0.21/46.8

## 5.4 Gamma Phase Decomposition

SEM analysis was performed to identify phase transformation or decomposition of gamma phase (body-centered cubic crystal structure) in as-cast and as-cast + homogenized samples. No gamma phase decomposition was observed in any as-received U-10Mo foils that were characterized using SEM.

## 5.5 Fuel Meat Thickness

The U-10Mo monolithic fuel fabrication process involves a number of complex material processing techniques such as casting, thermal annealing, hot and cold rolling, zirconium co-rolling, and HIP processing. The manufacturing process should consistently produce fuel with acceptable quality (i.e., that meets or exceeds design requirements) (Senor and Burkes 2014). Hence, it is important to verify the consistency of the fuel thickness produced during a typical fabrication process to support adequate irradiation performance.

The U-10Mo foil thickness was measured using BSE montage images obtained from an SEM microscope at 250× magnification for each specimen. Average thickness and standard deviation were calculated from the thickness data measured at each pixel. Summaries of the U-10Mo foil thicknesses for master foils, and 0.025 in and 0.010 in thick foils are shown in Table 19.

Table 19. Fuel meat thickness of U-10Mo specimens

Thickness (inch)	Processed Condition	Sample ID	Met ID	Direction	Avg. Thickness (μm)	SD (μm)	Avg. Thickness (in.)
0.047	Master foil	054-01-000 L	LEU2030	Long	1295	13	0.0509
			LEU2031	Trans	1284	27	0.0505
0.047	Master foil	054-01-000 M	LEU2032	Long	1265	10	0.0498
			LEU2033	Trans	1271	75	0.0500
0.047	Master foil	054-02-000 L	LEU2034	Long	1305.5	27.5	0.0514
			LEU2035	Trans	1315.9	18.2	0.0518
0.047	Master foil	054-02-000 M	LEU2043	Long	1268.4	18.8	0.0499
			LEU2044	Trans	1316.4	12.8	0.0518
0.047	Master foil	054-03-000 L	LEU2047	Long	1240.9	14.7	0.0488
			LEU2048	Trans	1296.9	35.1	0.0511
0.047	Master foil	054-03-000 M	LEU2045	Long	1264.0	14.0	0.0498
			LEU2046	Trans	1263.9	14.3	0.0498
0.047	Master foil	055-01-000 L	LEU2051	Long	1099.6	4.6	0.0433
			LEU2052	Trans	1177.3	25.6	0.0463
0.047	Master foil	055-01-000 M	LEU2053	Long	1137.9	10.1	0.0448
			LEU2055	Trans	1170	24.1	0.0461
0.047	Master foil	055-02-000 L	LEU2068	Long	1129	6.9	0.0444
			LEU2070	Trans	1103.1	16.8	0.0434
0.047	Master foil	055-02-000 M	LEU2067	Long	1107.5	10.2	0.0436
			LEU2069	Trans	1097.8	9.2	0.0432
0.025	Foil	054-01-001 L	LEU2021	Long	593	6	0.0233
			LEU2018	Trans	600	7	0.0236
0.025	Foil	054-01-002 M	LEU2024	Long	664	9	0.0261
			LEU2025	Trans	664	10	0.0261
0.025	Foil	054-02-001 L	LEU2026	Long	657.7	9.6	0.0259
			LEU2027	Trans	640.6	6.4	0.0252
0.025	Foil	054-02-002 M	LEU2028	Long	617.8	8.1	0.0243

Thickness (inch)	Processed Condition	Sample ID	Met ID	Direction	Avg. Thickness ( $\mu\text{m}$ )	SD ( $\mu\text{m}$ )	Avg. Thickness (in.)
0.025	Foil	054-03-001 L	LEU2029	Trans	614.3	6.6	0.0242
			LEU2022	Long	608.4	5.5	0.0239
			LEU2019	Trans	615.6	6.7	0.0242
0.025	Foil	054-03-002 M	LEU2023	Long	616.0	6.4	0.0242
			LEU2020	Trans	661.7	7.7	0.0261
0.010	Foil	055-01-001 L	LEU2036	Long	225.8	7.3	0.0089
			LEU2037	Trans	220.4	6.7	0.0087
0.010	Foil	055-01-002 M	LEU2049	Long	207.6	8.7	0.0081
			LEU2050	Trans	201.8	6.8	0.0079
0.010	Foil	055-02-001 L	LEU2057	Long	222.5	6.2	0.0088
			LEU2058	Trans	217.6	6.6	0.0086
0.010	Foil	055-02-001 M	LEU2054	Long	213.6	7.3	0.0084
			LEU2056	Trans	215.8	5.8	0.0085
0.025	Large foil	1MP-20-027 Center	LEU2072	Long	664.6	7.3	0.0262
			LEU2071	Trans	616.5	31.8	0.0243
		1MP-20-027 End	LEU2073	Long	780.9	8.4	0.0307
0.025	Large foil	2MP-20-027 Center	LEU2074	Trans	683.8	7.9	0.0269
			LEU2075	Long	616.6	20.6	0.0243
		2MP-20-027 End	LEU2076	Trans	630.4	20.1	0.0248
		LEU2077	Long	612.1	22.0	0.0241	
0.010	Large foil	1MP-20-0105 Center	LEU2078	Trans	597.9	79.3	0.0235
			LEU2083	Long	214.7	33.4	0.0084
		1MP-20-0105 End	LEU2084	Trans	211.5	26.8	0.0083
		LEU2085	Long	202.7	54.4	0.0080	
0.010	Large foil	2MP-20-0105 Center	LEU2086	Trans	215.3	25.6	0.0085
			LEU2079	Long	211.1	30.8	0.0083
		2MP-20-0105 End	LEU2080	Trans	211.7	32.3	0.0083
		LEU2081	Long	210.2	26.3	0.0083	
			LEU2082	Trans	216.9	18.7	0.0085

## 5.6 Zr Layer Thickness

The mechanical stability of the fuel-to-cladding interface is critical for maintaining satisfactory fuel performance. A method employed to mitigate this potential failure mode is to minimize the interaction between the U-10Mo fuel foil and the cladding by introducing a Zr interlayer. A barrier thickness of 25  $\mu\text{m}$  was selected to exceed the maximum fission fragment recoil range (about 9  $\mu\text{m}$  in Zr) and to allow for the inherent thickness variability resulting from the U-10Mo fuel fabrication process (Meyer et al. 2014). The starting microstructure and processing parameters need to be optimized properly to achieve the desired uniform Zr layers at the top and bottom of the U-10Mo fuel foil. Figure 13 shows representative Zr layers for a master foil (0.047 in. thick) as well as foils with 0.025 and 0.010 in. thickness. Microstructure shows Zr thinning in some of the regions in the master foil and the 0.025 in. foil. However, the Zr layer is

much more uniform in 0.010 in. thick foils. Figure 14 shows the representative microstructures of large foil specimens with 0.025 in. and 0.010 in. thick foils.

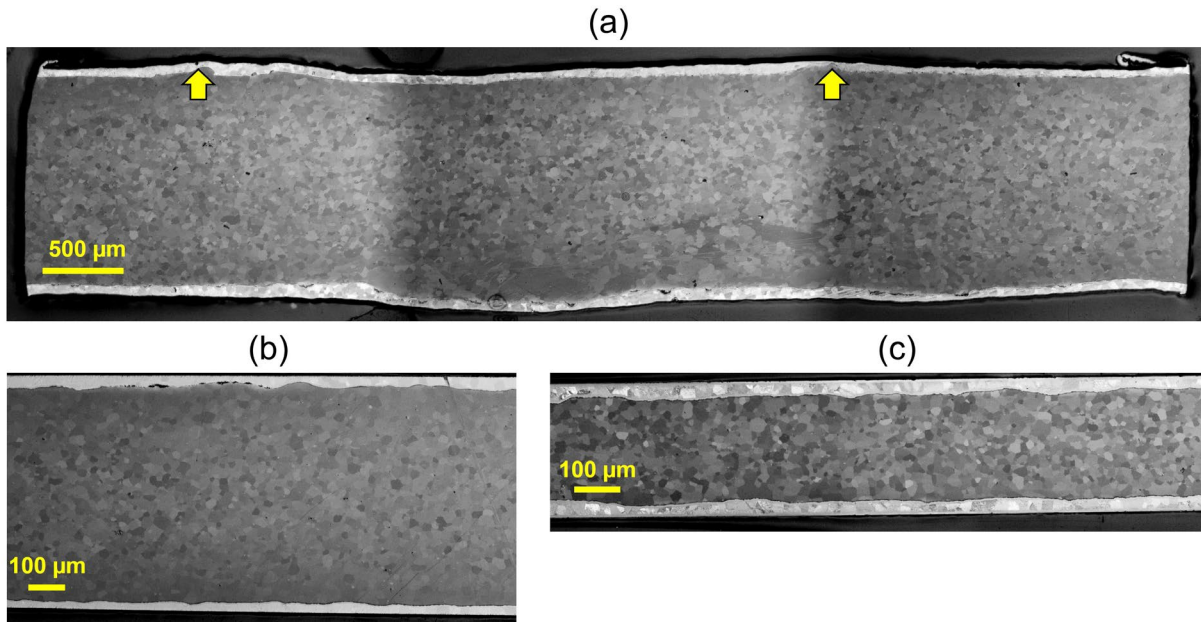


Figure 13. Typical Zr layers observed in U-10Mo foil specimens: (a) LEU-054-01-000-L Trans (0.047 in.), (b) LEU-054-01-001-L Long (0.025 in.), and (c) LEU-055-01-001-L Long (0.0105 in.).

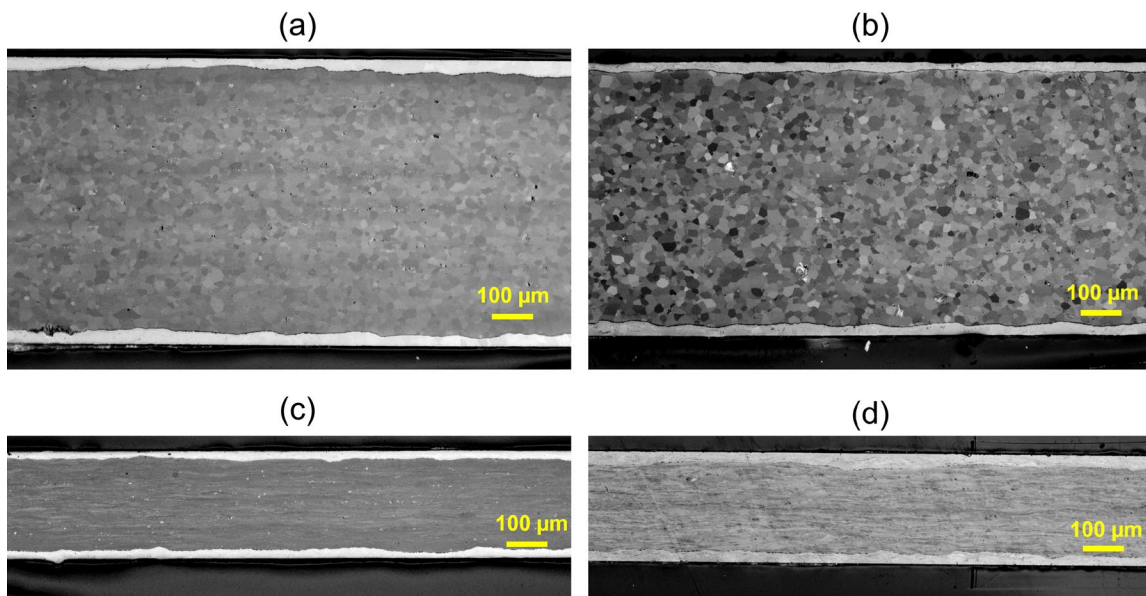


Figure 14. Typical Zr layers observed in U-10Mo large foil specimens: (a) 1MP-20-027 Center Long (0.025 in.), (b) 2MP-20-027 Center Long (0.025 in.), (c) 1MP-20-0105 Center Long (0.010 in.) and (d) 2MP-20-0105 Center Long (0.010 in.)

The Zr layer thickness in U-10Mo specimens was measured by using an SEI montage obtained from SEM. As with U-10Mo foil thickness measurement, an automated method was used to

measure thicknesses of top and bottom Zr layers. A summary of the Zr layer thicknesses for master foils as well as specimen foils is shown in Table 20. A summary plot shows that average Zr thicknesses for foils were approximately 88  $\mu\text{m}$ , 25  $\mu\text{m}$ , and 25  $\mu\text{m}$  for U 10Mo specimens of 0.047 in., 0.025 in., and 0.010 in. thicknesses, respectively (Figure 15).

Table 20. Summary of the Zr layer (top and bottom) thicknesses for U-10Mo specimens

Thickness (inch)	Processing Condition	Sample ID	Met ID	Direction	Top Zr Layer		Bottom Zr Layer	
					Avg. Thickness ( $\mu\text{m}$ )	SD ( $\mu\text{m}$ )	Avg. Thickness ( $\mu\text{m}$ )	SD ( $\mu\text{m}$ )
0.047	Master foil	054-01-000 L	LEU2030	Long	49.4	6.0	60.3	7.0
			LEU2031	Trans	60.8	13.2	48.3	6.2
0.047	Master foil	054-01-000 M	LEU2032	Long	49.2	3.6	48.9	5.2
			LEU2033	Trans	44.9	10.1	52.3	7.5
0.047	Master foil	054-02-000 L	LEU2034	Long	42.9	7.1	27.7	6.0
			LEU2035	Trans	54.2	13.6	55.3	5.0
0.047	Master foil	054-02-000 M	LEU2043	Long	45.6	7.4	46.3	11.9
			LEU2044	Trans	44.2	7.4	32.8	8.1
0.047	Master foil	054-03-000 L	LEU2047	Long	43.4	8.2	45.9	4.8
			LEU2048	Trans	56.5	8.6	36.3	11.7
0.047	Master foil	054-03-000 M	LEU2045	Long	63.5	4.1	50.0	9.1
			LEU2046	Trans	48.7	11.6	55.3	5.0
0.047	Master foil	055-01-000 L	LEU2051	Long	164.9	5.7	177.1	3.8
			LEU2052	Trans	125.7	11.1	142.0	8.8
0.047	Master foil	055-01-000 M	LEU2053	Long	157.1	2.0	161.6	4.1
			LEU2055	Trans	138.7	2.0	122.4	1.7
0.047	Master foil	055-02-000 L	LEU2068	Long	125.7	1.6	133.8	2.1
			LEU2070	Trans	175.6	0.9	160.1	0.9
0.047	Master foil	055-02-000 M	LEU2067	Long	137.3	1.8	144.0	1.3
			LEU2069	Trans	170.7	0.5	129.1	0.5
0.025	Foil	054-01-001 L	LEU2021	Long	24.1	4.1	26.8	5.7
			LEU2018	Trans	35.7	5.4	28.3	5.0
0.025	Foil	054-01-002 M	LEU2024	Long	20.7	6.1	19.9	5.1
			LEU2025	Trans	27.2	4.5	14.4	6.7
0.025	Foil	054-02-001 L	LEU2026	Long	20.9	6.8	27.9	11.6
			LEU2027	Trans	25.9	4.8	14.2	5.5
0.025	Foil	054-02-002 M	LEU2028	Long	22.3	5.7	27.9	9.0
			LEU2029	Trans	28.2	5.0	17.5	4.6

Thickness (inch)	Processing Condition	Sample ID	Met ID	Direction	Top Zr Layer		Bottom Zr Layer	
					Avg. Thickness ( $\mu\text{m}$ )	SD ( $\mu\text{m}$ )	Avg. Thickness ( $\mu\text{m}$ )	SD ( $\mu\text{m}$ )
0.025	Foil	054-03-001 L	LEU2022	Long	20.6	4.0	19.6	6.4
			LEU2019	Trans	23.5	7.7	20.2	4.3
0.025	Foil	054-03-002 M	LEU2023	Long	26.7	6.9	19.4	3.7
			LEU2020	Trans	26.6	6.3	25.1	5.4
0.010	Foil	055-01-001 L	LEU2036	Long	17.0	6.4	29.6	5.1
			LEU2037	Trans	30.6	5.8	26.5	3.9
0.010	Foil	055-01-002 M	LEU2049	Long	24.0	2.9	14.0	10.0
			LEU2050	Trans	26.0	3.8	19.0	3.6
0.010	Foil	055-02-001 L	LEU2057	Long	28.0	0.4	21.9	2.5
			LEU2058	Trans	24.7	3.5	25.0	1.8
0.010	Foil	055-02-001 M	LEU2054	Long	28.9	10.4	27.9	5.1
			LEU2056	Trans	33.8	8.7	23.8	1.6
0.025	Large foil	1 MP-20-027 Center	LEU2072	Long	23.4	3.6	22.2	4.2
			LEU2071	Trans	27.7	5.5	26.5	4.8
		1 MP-20-027 End	LEU2073	Long	25.0	8.6	28.2	9.7
			LEU2074	Trans	28.4	5.2	23.7	5.8
0.025	Large foil	2MP-20-027 Center	LEU2075	Long	24.7	4.8	23.1	4.2
			LEU2076	Trans	26.2	4.4	22.6	4.2
		2MP-20-027 End	LEU2077	Long	23.0	4.4	25.0	6.0
			LEU2078	Trans	26.6	6.6	21.8	7.0
0.010	Large foil	1MP-20-0105 Center	LEU2083	Long	30.6	6.0	18.23	3.3
			LEU2084	Trans	30.6	6.0	26.8	2.6
		1MP-20-0105 End	LEU2085	Long	37.4	7.9	29.3	4.5
			LEU2086	Trans	29.1	4.4	29.2	5.9
0.010	Large foil	2MP-20-0105 Center	LEU2079	Long	19.8	3.1	28.9	2.6
			LEU2080	Trans	28.9	2.0	22.3	12.7
		2MP-20-0105 End	LEU2081	Long	33.1	6.3	40.6	8.0
			LEU2082	Trans	29.6	4.0	26.6	3.8

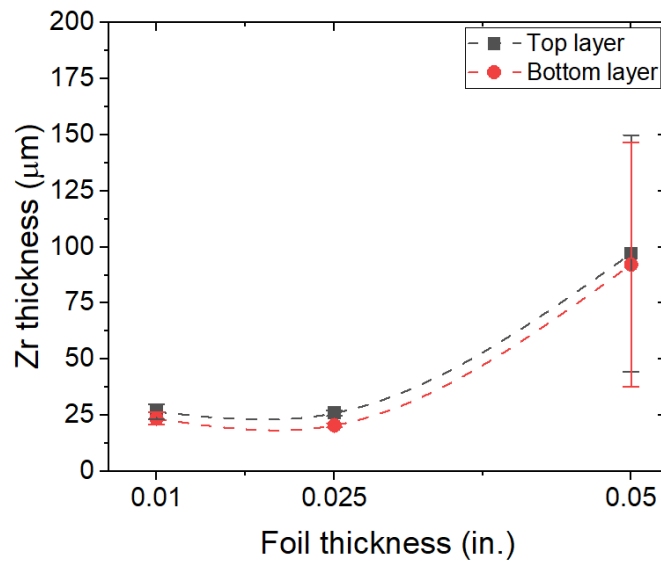


Figure 15. Zr thickness variation of Zr layer thickness with thickness reduction

To study the interface between U-10Mo and Zr layers, interaction layer thickness was measured. For representative purposes, typical U-10Mo–Zr interaction layers observed in U-10Mo specimens are shown in Figure 16. The average thickness of the interaction layer was approximately 1.5–2.0 μm. The interaction layer is basically a U-Zr intermetallic phase. Single or multiple phases could be present in the interaction layer. The interaction layer had a wavy cross section, and its thickness varied throughout the individual specimen.

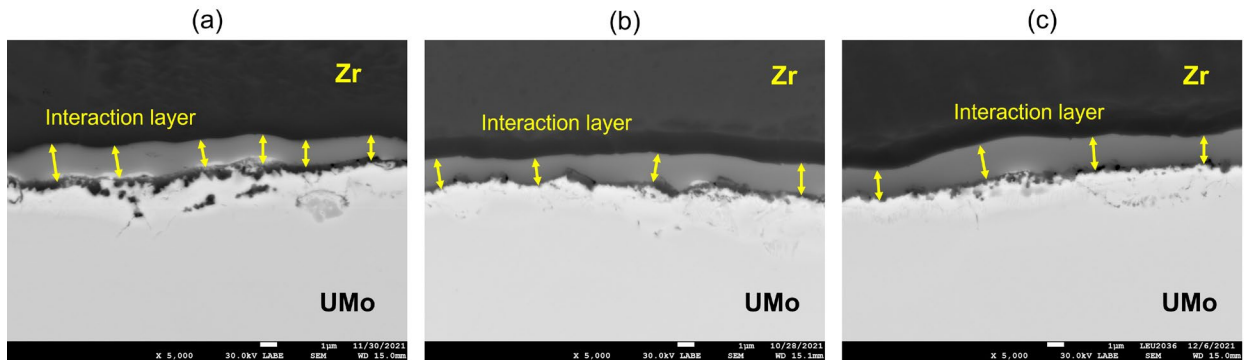


Figure 16. Representative interaction layers observed in U-10Mo specimens : (a) LEU-054-01-000-L Long (0.047 in.), (b) LEU-054-01-001-L Long (0.025 in.), and (c) LEU-055-01-001-L Long (0.010 in.)

## 6.0 Conclusions

PNNL received as-cast and foil samples with Zr layers (0.047 in. thick hot-rolled and annealed, 0.025 in. thick cold-rolled and annealed, and 0.010 in. thick cold-rolled and annealed) from BWXT. Along with those, four plates (0.025 in. and 0.010 in. thick) with Zr layers were also received. Characterizations were performed on all the cast and foil specimens.

The report describes the results of PNNL analyses of MP-2 fuel characterization samples. Microstructure, chemical composition, U-10Mo foil thickness, and Zr thickness were evaluated in both the longitudinal and transverse directions for foils of different thicknesses.

The following conclusions were drawn from the above investigations:

- In as-cast PD-STD2 specimens, the average grain size was in the range of 130–417  $\mu\text{m}$ . Dendritic structure was observed in some of the cast samples. After homogenization, the grain size remained almost the same for both the cast samples. However, dendritic structure was not observed in homogenized samples.
- The U-10Mo average grain size decreased as the foil thickness decreased. The average grain sizes observed in U-10Mo samples were 16  $\mu\text{m}$  for 0.010 in. thickness, 18  $\mu\text{m}$  for 0.025 in. thickness, and 27  $\mu\text{m}$  for 0.047 in. thickness. These are plotted in Figure 17.

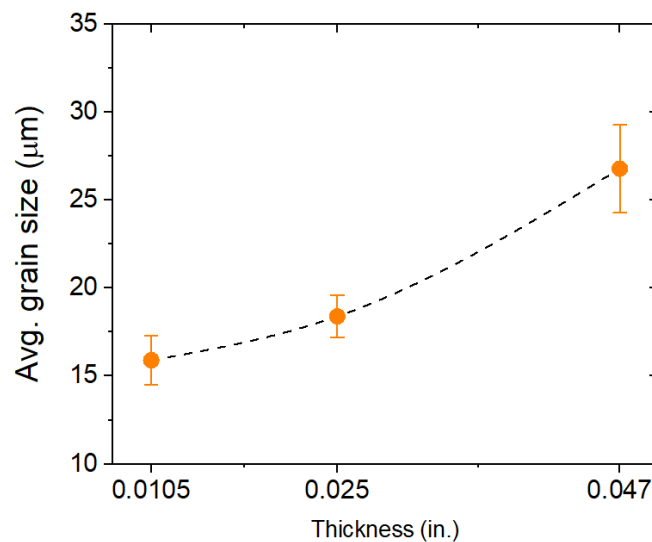


Figure 17. Average grain size ranges for different thickness U-10Mo master foils, and 0.025 in. and 0.010 in. thick foils

- In as-cast samples, Mo inhomogeneity was observed inside dendrite arm regions. This Mo inhomogeneity resulted in a standard deviation of Mo content above 0.5 (wt%) in some of the as-cast samples. However, after homogenization, Mo variation decreased below 0.5 (wt%). The microstructures of all foil samples showed nearly homogeneous Mo distribution and no chemical banding was observed. The standard deviation of Mo content was less than 0.5 (wt%) in all foils.
- In as-cast samples, average carbide fraction was under 1.5%, whereas in foils, average carbide fraction was less than 1.0%. In as-cast samples, average carbide size was in the range of 11–25  $\mu\text{m}^2$ . Average carbide sizes for 0.47 in., 0.025 in., and 0.010 in. foils were in

the ranges of 5–13  $\mu\text{m}^2$ , 3–11  $\mu\text{m}^2$ , and 3–5  $\mu\text{m}^2$ , respectively. Carbide particles were fragmented significantly with thickness reduction.

- No gamma phase decomposition was observed in any of the as-received specimens that were characterized using scanning electron microscopes.
- Analyses of Zr thickness (top and bottom layers) showed large thickness variations in all U-10Mo master foils. However, Zr layers in 0.025 and 0.010 in. foils were very uniform. The average Zr thicknesses (top/bottom) were approximately 88  $\mu\text{m}$ , 25  $\mu\text{m}$ , and 25  $\mu\text{m}$  for U-10Mo specimens of thicknesses 0.047 in., 0.025 in., and 0.010 in., respectively. Similarly, in large foils, average thicknesses of Zr layers for 0.025 in., and 0.010 in. foils were both approximately 25  $\mu\text{m}$ .
- The average thickness of the interaction layer in U-10Mo specimens was approximately 1.5–2.0  $\mu\text{m}$ . The interaction layer is basically a U-Zr intermetallic phase. Single or multiple phases could be present in the interaction layer. The interaction layer was wavy, and its thickness varied throughout individual specimens.
- Orientation-based imaging using EBSD was carried out to examine the microstructural state (deformed or recrystallized) and calculate grain size of master foil and foils. The grains were equiaxed and fully recrystallized. No abnormal grain growth was observed. The grain sizes calculated from optical microstructure observation and EBSD are comparable. The trend of grain size evolution with thickness reduction is very similar in both the measurement methods.

## 7.0 Quality Assurance

This work was performed in accordance with the Pacific Northwest National Laboratory (PNNL) Nuclear Quality Assurance Program (NQAP). The NQAP complies with the United States Department of Energy Order 414.1D, *Quality Assurance*. The NQAP uses NQA-1-2012, *Quality Assurance Requirements for Nuclear Facility Application* as its consensus standard and NQA-1-2012 Subpart 4.2.1 as the basis for its graded approach to quality.

This work emphasized acquiring new theoretical or experimental knowledge. The information associated with this report should not be used as design input or operating parameters without additional qualification.

## 8.0 References

- Bostrom, W., and E. Halteman. 1956. *The Metastable Gamma Phase in Uranium Base Molybdenum Alloys*. Westinghouse Electric Corporation WAPD-T-415. Pittsburgh, Pennsylvania: W. E. Corporation. <https://www.osti.gov/scitech/biblio/4347373>.
- Burkes, D. E., R. Prabhakaran, T. Hartmann, J.-F. Jue, and F. J. Rice. 2010. "Properties of Du-10wt% Mo Alloys Subjected to Various Post-Rolling Heat Treatments." *Nuclear Engineering and Design* 240 (6): 1332-1339. <https://doi.org/10.1016/j.nucengdes.2010.02.008>.
- Cheng, G., X. Hu, W. E. Frazier, C. A. Lavender, and V. V. Joshi. 2018. "Effect of Second Phase Particles and Stringers on Microstructures after Rolling and Recrystallization." *Materials Science and Engineering: A* 736: 41-52. <https://doi.org/10.1016/j.msea.2018.08.040>.
- Hu, X., X. Wang, V. V. Joshi, and C. A. Lavender. 2018. "The Effect of Thermomechanical Processing on Second Phase Particle Redistribution in U-10wt%Mo." *Journal of Nuclear Materials* 500: 270-279. <https://doi.org/10.1016/j.jnucmat.2017.12.042>.
- INL. 2021. *Characterization Plan for the Fabrication of U-10mo Plate Fuel for Ushpr- Fuel Fabrication Pillar*. Idaho National Laboratory PLN-6329 R0. 4. Idaho Falls, ID.
- Jana, S., A. Devaraj, L. Kovarik, B. Arey, L. Sweet, T. Varga, C. Lavender, and V. Joshi. 2017. "Kinetics of Cellular Transformation and Competing Precipitation Mechanisms During Sub-Eutectoid Annealing of U10mo Alloys." *Journal of Alloys and Compounds* 723: 757-771. <https://doi.org/10.1016/j.jallcom.2017.06.292>.
- Joshi, V. V., E. A. Nyberg, C. A. Lavender, D. Paxton, and D. E. Burkes. 2015. "Thermomechanical Process Optimization of U-10wt% Mo – Part 2: The Effect of Homogenization on the Mechanical Properties and Microstructure." *Journal of Nuclear Materials* 465: 710-718. <https://doi.org/10.1016/j.jnucmat.2015.07.005>.
- Meyer, M. K., J. Gan, J. F. Jue, D. D. Keiser, E. Perez, A. Robinson, D. M. Wachs, N. Woolstenhulme, G. L. Hofman, and Y. S. Kim. 2014. "Irradiation Performance of U-Mo Monolithic Fuel." *Nuclear Engineering and Technology* 46 (2): 169-182. <https://doi.org/10.5516/Net.07.2014.706>.
- Nyberg, E., V. V. Joshi, C. Lavender, D. M. Paxton, and D. E. Burkes. 2013. *The Influence of Casting Conditions on the Microstructure of as-Cast U-10mo Alloys: Characterization of the Casting Process Baseline*. Pacific Northwest National Laboratory PNNL-23049. Richland, Washington. [https://www.pnnl.gov/main/publications/external/technical\\_reports/PNNL-23049.pdf](https://www.pnnl.gov/main/publications/external/technical_reports/PNNL-23049.pdf).
- Nyberg, E. A., V. V. Joshi, C. A. Lavender, D. M. Paxton, and D. E. Burkes. 2014. *Influence of Homogenization on the Mechanical Properties and Microstructure of the U-10mo Alloy*. Pacific Northwest National Laboratory PNNL-23348. Richland, Washington. [https://www.pnnl.gov/main/publications/external/technical\\_reports/PNNL-23348.pdf](https://www.pnnl.gov/main/publications/external/technical_reports/PNNL-23348.pdf).
- Prabhakaran, R., V. V. Joshi, M. A. Rhodes, A. L. Schemer-Kohn, A. Guzman, and C. A. Lavender. 2016. *U-10mo Sample Preparation and Examination Using Optical and Scanning Electron Microscopy*. Pacific Northwest National Laboratory PNNL-25308, Rev. 1. Richland, Washington.

[https://www.pnnl.gov/main/publications/external/technical\\_reports/PNNL-25308Rev1.pdf](https://www.pnnl.gov/main/publications/external/technical_reports/PNNL-25308Rev1.pdf).

Senor, D. J., and D. Burkes. 2014. *Fuel Fabrication Capability Research and Development Plan*. Pacific Northwest National Laboratory PNNL-22528, Rev. 1. Richland, Washington. [https://www.pnnl.gov/main/publications/external/technical\\_reports/pnnl-22528.pdf](https://www.pnnl.gov/main/publications/external/technical_reports/pnnl-22528.pdf).

# **Pacific Northwest National Laboratory**

902 Battelle Boulevard  
P.O. Box 999  
Richland, WA 99354

1-888-375-PNNL (7665)

***[www.pnnl.gov](http://www.pnnl.gov)***